

1    The Role of Naphthalene and Its Derivatives in the  
2    Formation of Secondary Organic Aerosols in the  
3    Yangtze River Delta Region, China

4    *Fei Ye<sup>1</sup>, Jingyi Li<sup>1</sup>, Yaqin Gao<sup>2</sup>, Hongli Wang<sup>2</sup>, Jingyu An<sup>2,3</sup>, Cheng Huang<sup>2</sup>, Song Guo<sup>4</sup>, Keding  
5    Lu<sup>4</sup>, Kangjia Gong<sup>1</sup>, Haowen Zhang<sup>1</sup>, Momei Qin<sup>1</sup>, Jianlin Hu<sup>1</sup>*

6    <sup>1</sup> Jiangsu Key Laboratory of Atmospheric Environment Monitoring and Pollution Control,  
7    Collaborative Innovation Center of Atmospheric Environment and Equipment Technology, School  
8    of Environmental Science and Engineering, Nanjing University of Information Science &  
9    Technology, Nanjing, 210044, China

10    <sup>2</sup> State Environmental Protection Key Laboratory of the Formation and Prevention of Urban Air  
11    Pollution Complex, Shanghai Academy of Environmental Sciences, Shanghai 200233, China

12    <sup>3</sup> Shanghai Key Laboratory of Atmospheric Particle Pollution and Prevention, Department of  
13    Environmental Science and Engineering, Fudan University, Shanghai 200438, China

14    <sup>4</sup> State Key Joint Laboratory of Environmental Simulation and Pollution Control, College of  
15    Environmental Sciences and Engineering, Peking University, Beijing, 100871, China

16    Correspondence **to:** Jingyi Li (jingyili@nuist.edu.cn), Jianlin Hu (jianlinhu@nuist.edu.cn)

17

18 **Abstract.** Naphthalene (Nap) and its derivatives, including 1-methylnaphthalene (1-MN) and 2-methylnaphthalene (2-MN), serve as prominent intermediate volatile organic compounds (IVOCs) contributing to the formation of secondary organic ~~carbon (SOC)~~aerosol (SOA). In this study, the Community ~~Multi-Scale~~Multiscale Air Quality (CMAQ) model coupled with detailed emissions and reactions of these compounds was utilized to examine their roles in the formation of ~~SOC~~SOA and other secondary pollutants in the Yangtze River Delta (YRD) region during summer.

24 ~~Remarkably, significant~~Significant underestimations of Nap and MN concentrations (by 79% and 85%) were observed at the Taizhou site. ~~To better capture the temporal variations based on the model results using the default emissions. Constrained by the observations, anthropogenic emissions of Nap and MN, their emissions in the YRD~~entire region were ~~scaled up~~multiplied by a factor of 5 and 7, respectively, ~~with constraints based on field measurements. After adjusting their emissions, to better capture the evolution of pollutants. The average concentration of Nap concentrations~~ reached ~~27.25~~27.25 ppt in the YRD, ~~accounting for with Nap contributing~~accounting for 4.1% and ~~98.1%~~13.712.6% (up to ~~13.712.6%~~13.712.6%) of total ~~aromatic~~aromatic emissions and aromatic-derived ~~secondary organic carbon (SOC)~~secondary organic carbon (SOC), respectively. The concentrations of 1-MN and 2-MN were relatively low, ~~with an average of 3 and 6 averaging at 2 ppt in the YRD, and contributed 3.15 ppt. Together, they accounted for only 2.4% of the aromatic-derived SOC. The influences impacts of Nap and MN oxidation on ozone and radicals might be trivial on a~~were insignificant at regional scale scales but were not negligible when considering daily fluctuations, ~~particularly in Shanghai~~locations with high emissions of Nap and Suzhou MN. This study ~~emphasizes the high SOC~~highlights the significant roles of Nap and MN in the formation ~~potentials of Nap and MN~~SOA, which may pose environmental risks and adverse health effects.

## 40 1 Introduction

41 Secondary organic aerosols (SOA) are formed from the condensation and multiphase  
42 evolution of less volatile organic compounds (VOCs), which can be directly emitted or produced  
43 from the oxidation of higher volatile organics in the atmosphere. SOA not only affects visibility  
44 and human health but also ~~has impacts~~exerts direct effects on the climate ~~directly~~ by absorbing  
45 and reflecting solar radiation ~~and indirectly, as well as~~ indirect effects by ~~affecting~~influencing  
46 cloud formation ([Chen et al., 2016; Zhang and Ying, 2012](#))[\(Chen et al., 2016; Zhang and Ying,](#)  
47 [2012\)](#). Semi-volatile and intermediate-volatile organic compounds (S/IVOCs) have been identified  
48 as the key precursors of SOA (Robinson et al., 2007; Hu et al., 2022). IVOCs are categorized by  
49 small polycyclic aromatic hydrocarbons (PAHs), intermediate-length alkanes (e.g. ~~n-hexadecane~~),  
50 ~~and phenols~~[\(Pye and Seinfeld, 2010\)](#)[n-hexadecane](#), ~~and phenols~~[\(Pye and Seinfeld, 2010\)](#). PAHs  
51 are organic compounds containing multiple aromatic rings. [In 2004](#), China ~~was responsible for~~  
52 [exhibited](#) the highest annual PAH emissions ~~at (114 Gg with a portion of)~~ [globally, accounting](#)  
53 [for 22% of global](#)~~the~~ [total PAH](#) [emissions in 2004](#)[\(Zhang and Tao, 2009\)](#)[worldwide](#) [\(Zhang and](#)  
54 [Tao, 2009\)](#). Naphthalene (Nap) and methylnaphthalene (MN), such as 1-methylnaphthalene (1-  
55 MN) and 2-methylnaphthalene (2-MN), are the most abundant airborne PAHs (Chen et al., 2016;  
56 Fang et al., 2021), ~~which are mainly primarily~~ emitted from ~~the~~ combustion of fossil fuels, biomass  
57 burning, and industrial sectors ([Fang et al., 2021](#))[\(Fang et al., 2021\)](#).

58 ~~Chamber studies have identified the gas and particle phase products from Nap reacting with~~  
59 ~~hydroxyl radical (OH)~~ ([Huang et al., 2019](#)). ~~Ring retaining products (e.g., 1,4-naphthoquinone)~~  
60 ~~with lower volatilities are dominant under low nitrogen oxide (NO<sub>x</sub>) conditions, and ring opening~~  
61 ~~products (e.g., 2-formylcinnamaldehyde) with higher volatilities are dominant in the presence of~~  
62 ~~high NO<sub>x</sub>. Chan et al. (2009) evaluated the SOA yields of Nap, 1-MN, 2-MN, and 1,2-dimethyl~~  
63 ~~naphthalene in chambers and applied these yields to estimate SOA formation from primary~~

64 ~~emissions of diesel engines and wood burning. The SOA yields were 55–75% under low NO<sub>x</sub>~~  
65 ~~conditions at a total organic aerosol loading of 15 μg m<sup>-3</sup>, which was more efficient than high NO<sub>x</sub>~~  
66 ~~conditions (25–45%). In the photo-oxidation period of less than 12 h, these PAHs produced 3–5~~  
67 ~~times more SOA than light aromatic compounds and were responsible for up to 54% of total SOA~~  
68 ~~from the oxidation of diesel emissions. Huang et al. (2019) applied a tracer method and discovered~~  
69 ~~that 14.9% of SOA was owing to the oxidation of Nap and MN in the afternoon during the~~  
70 ~~wintertime haze in Beijing. Shakya and Griffin (2010) also reported 36–162 kg day<sup>-1</sup> of SOA~~  
71 ~~production from the mobile source emitted PAHs (including Nap, 1-MN, and 2-MN) in Houston~~  
72 ~~based on the yields from their study and that of Chan et al. (2009). Based on the yield from Shakya~~  
73 ~~and Griffin (2010), Liu et al. (2015) showed that Nap contributed 8–52% of the total SOA~~  
74 ~~originating from benzene, toluene, C2 benzene, C3 benzene, C4 benzene, and Nap in light-duty~~  
75 ~~gasoline vehicle exhausts. All these experimental findings demonstrate the significant role of Nap~~  
76 ~~and MN in SOA formation in the environment with anthropogenic influences dominated. However,~~  
77 ~~these results might not accurately reflect the actual atmospheric conditions due to the simplicity of~~  
78 ~~reaction conditions and the limited precursors involved in chamber studies. Chamber studies have~~  
79 identified the gas- and particle-phase products from Nap reacting with hydroxyl radicals (OH<sup>·</sup>)  
80 (Huang et al., 2019). Ring-retaining products (such as 1,4-naphthoquinone) with lower volatilities  
81 dominate under conditions of low nitrogen oxides (NO<sub>x</sub>), and ring-opening products (such as 2-  
82 formyl cinnamaldehyde) with higher volatilities dominate in the presence of high NO<sub>x</sub>. Chan et al.  
83 (2009) evaluated the SOA yields of Nap, 1-MN, 2-MN, and 1,2-dimethyl naphthalene in chambers  
84 to estimate SOA formation from primary emissions of diesel engines and wood burning. It was  
85 found that SOA is more efficiently produced under low-NO<sub>x</sub> conditions than high-NO<sub>x</sub> conditions,  
86 with yields of 55–75% and 25–45%, respectively, at a total organic aerosol loading of 15 μg m<sup>-3</sup>.

During photo-oxidation of less than 12 h, these PAHs produced 3–5 times more SOA than light aromatic compounds, accounting for up to 54% of the total SOA from the oxidation of diesel emissions. Huang et al. (2019) applied a tracer method to determine that 14.9% of SOA was attributed to the oxidation of Nap and MN in the afternoon during wintertime haze in Beijing. Shakya and Griffin (2010) also reported 37–162 kg day<sup>-1</sup> of SOA production from the mobile source emitted PAHs (including Nap, 1-MN, and 2-MN) in Houston, based on the yields from their study and that of Chan et al. (2009). By adopting the SOA yields from Shakya and Griffin (2010), Liu et al. (2015) showed that Nap accounted for 8–52% of the total SOA derived from benzene, toluene, C2-benzene, C3-benzene, C4-benzene, and Nap in exhaust emissions from light-duty gasoline vehicles. All these experimental findings demonstrate the significant role of Nap and MN in SOA formation in environments dominated by anthropogenic influences. However, these results might not accurately reflect the actual atmospheric conditions due to the simplicity of reaction conditions and the limited precursors involved in chamber studies (Ling et al., 2022).

Numerical models have been developed and utilized to assess the contribution of S/IVOCs to SOA (Hayes et al., 2015; Pye and Seinfeld, 2010; An et al., 2023). Zhang and Ying (2011) showed that PAHs emitted from anthropogenic sources could produce SOA mass as much as 10% of that from the traditional light aromatics or around 4% of total anthropogenic SOA by using the Community Multiscale Air Quality (CMAQ) model. However, the products from several explicit PAH species (Nap, MN, dimethyl naphthalene, ethyl naphthalene, acenaphthylene, acenaphthene, fluorene, phenanthrene, fluoranthene) were lumped rather than separated for their contributions to SOA due to limited experimental data. Pye and Poulton (2012) utilized the CMAQ model and tracked 10% of peroxy radicals produced from the ARO2 (lumped aromatics in CMAQ) and OH<sup>+</sup> reaction as for that of Nap without considering the emissions and the accurate OH<sup>+</sup> reactivity of

110 Nap. According to Cohan et al. (2013), the modeled SOA increased by roughly 1–10% when Nap  
111 emissions from on-road gasoline and diesel vehicles were considered. Their simulations showed a  
112 lower bound in the SOA production from Nap due to underestimations in the emission inventory  
113 in the South Coast Air Basin of California. Majdi et al. (2019) found that Nap and MN contributed  
114 2.4% to the total organic aerosol (OA) originating from wildfires over the Euro-Mediterranean  
115 region during the summer of 2007 by using a 3D chemistry-transport model (CTM). The  
116 contributions of Nap and MN to SOA over a regional scale in China had not been quantified.

117 Zhang and Ying (2011) showed that PAHs emitted from anthropogenic sources could  
118 produce SOA mass as much as 10% of that from the traditional light aromatics or approximately  
119 4% of the total anthropogenic SOA by using the Community Multiscale Air Quality (CMAQ)  
120 model. However, the SOA products of several PAH species such as Nap and MN were lumped  
121 together due to limited experimental data for explicit parameterization. Pye and Pouliot (2012)  
122 assumed that 10% of ARO2 (lumped aromatic species) reacted with OH<sup>·</sup> to represent SOA  
123 formation from PAHs in the CMAQ model, using Nap as a surrogate for parameterization, without  
124 considering individual PAH's emissions and OH<sup>·</sup> reactivity. According to Cohan et al. (2013), the  
125 modeled SOA increased by roughly 1–10% when Nap emissions from on-road gasoline and diesel  
126 vehicles were considered. Their simulations showed a lower limit in the SOA production from  
127 Nap due to underestimations in the emission inventory in the South Coast Air Basin of California.  
128 Majdi et al. (2019) found that Nap and MN contributed 2.4% of the total organic aerosol (OA)  
129 originating from wildfires over the Euro-Mediterranean region during the summer of 2007 by  
130 using a 3D chemical-transport model (CTM). The contributions of Nap and MN to SOA at regional  
131 scales in China had not been quantified.

132 In this study, SOA formation from Nap, 1-MN, and 2-MN in the Yangtze River Delta (YRD)  
133 region during the EXPLORE-YRD -(EXPeriment on the eLucidation of the atmospheric Oxidation  
134 capacity and aerosol foRmation, and their Effects in the Yangtze River Delta) campaign period  
135 (May 20 – June 18, 2018) was investigated withby using an updated CMAQ model that  
136 incorporated explicit SOA schemes for these PAHs. Emission inventories of Nap, 1-MN, and 2-  
137 MN were estimated based on different sources and methods and validated against observations.  
138 After that, the influences of Nap and MN on secondary organic carbon (SOC), ozone (O<sub>3</sub>), and  
139 radical concentrations were examined in the locations with high concentrationslevels of Nap and  
140 MN as well as at the regional scalewere examined separately. The newly added SOA  
141 parameterizations for 1-MN and 2-MN were fitted by both two-product and one-product methods  
142 to compare the differences. We findfound that Nap and its derivatives, although accounting for a  
143 small fraction of emitted aromatics (5.1%), contributed 12.410.4 % of aromatic-derived SOC in the  
144 YRD.

## 145 **2 Methods**

### 146 **2.1 Modified SOA formation pathways of MN**

147 The CMAQ model version 5.2, coupled with the SAPRC07tic atmospheric chemical  
148 mechanism and the AERO6i aerosol module, was updated to include the oxidation of 1-MN and  
149 2-MN by OH<sup>·</sup> and the corresponding SOA formation pathways. In the original CMAQ model, Nap  
150 reacts with OH<sup>·</sup> to form SOA under lowhigh- and highlow-NO<sub>x</sub> conditions, which are represented  
151 by two different counter species PAHNRXN and PAHHRXNand PAHNRXN, respectively (Fig.  
152 S11a). Similar to Nap, 1-MN, and 2-MN were treated explicitly treated as reacting with OH<sup>·</sup> and  
153 forming SOA counter species under high NO<sub>x</sub> (aMPAHRXN and bMPAHRXN) and low NO<sub>x</sub>  
154 (aMPAHRXN and bMPAHRXN), along with other products following Zhang and Ying

155 (2012). [Zhang and Ying \(2012\)](#). These counter species were used to calculate the production of  
156 SOA through gas-particle partitioning based on yields ( $\alpha_i$ ) and partitioning coefficients ( $K_{\text{om},i}$ ,  $\text{m}^3$   
157  $\mu\text{g}^{-1}$ ) of condensable organic products derived from chamber experiment data. ~~The detailed~~  
158 ~~descriptions~~[Details](#) of gas-particle partitioning ~~to fit for fitting~~ SOA ~~yield through formation using~~  
159 one-product and two-product methods are ~~depicted~~[described](#) in the Supplement.

160 ~~In gas-particle partitioning of~~[In](#) the original CMAQ model, a two-product method (SV\_PAH1  
161 and SV\_PAH2) was used to represent the SOA formation from Nap under high- $\text{NO}_x$  conditions,  
162 ~~which are~~ denoted as APAH1J and APAH2J, respectively (Fig. [S1a1a](#)). Under low- $\text{NO}_x$  conditions,  
163 a one-product method was used to represent the SOA formation from Nap, denoted as APAH3J.  
164 It was assumed that APAH3J ([with](#) a yield of  $\alpha_3$ ) was non-volatile and resided in the particle phase.  
165 Similar to Nap, a two-product method for the ~~oxidation products of~~[SOA formation from](#) 1-MN  
166 ~~was added~~ under high- $\text{NO}_x$  conditions [was added](#) as shown in Fig. [S1b1b](#), with the SOA species  
167 denoted as AaMPAH1J and AaMPAH2J. ~~A~~[Additionally, a](#) one-product method ~~to~~  
168 ~~characterize~~[characterizing](#) the ~~oxidation products of~~[SOA formation from](#) 1-MN ~~under high- $\text{NO}_x$~~   
169 ~~conditions~~ ~~was also~~ applied to compare ~~the difference~~[differences](#) caused by ~~the~~[different](#) fitting  
170 ~~approach~~[approaches](#). As shown in Fig. [S1e1c](#), the semi-volatile organic product SV\_aMPAH1'  
171 undergoes equilibrium partitioning to form SOA (AaMPAH1J'). Under low- $\text{NO}_x$  conditions, a  
172 non-volatile SOA product AaMPAH3J is formed ~~by the through~~ oxidation of 1-MN. The SOA  
173 ~~pathways~~[scheme](#) of 2-MN ~~follow followed that of~~ 1-MN, with ~~the~~ corresponding ~~SOA~~ products  
174 ~~of~~[AbMPAH1J, and](#) AbMPAH2J, ~~(or AbMPAH1J')~~ ~~under high- $\text{NO}_x$  conditions~~ and AbMPAH3J  
175 ~~under low- $\text{NO}_x$  conditions~~, respectively. ~~In addition~~[Moreover](#), all semi-volatile SOA products  
176 ~~originating from~~ [MN](#) undergo condensed-phase oligomerization reactions at the same rate ~~of as~~  
177 APAH1J and APAH2J ~~and produce~~, [generating anthropogenic](#) non-volatile oligomers (AOLGAJ)

178 ~~that belong to the anthropogenic source.).~~ Other processes and parameters involved in the newly  
179 added SOA pathways for 1-MN and 2-MN, such as the dry and wet deposition and the molecular  
180 weight of the oxidation products<sub>2</sub> were set to be the same as Nap due to limited experimental data.  
181 Details of all the parameters, i.e.,  $\alpha_i$ ,  $K_{\text{om},i}$ , and  $\Delta H_{\text{vap},i}$  are summarized in Table S1.

## 182 2.2 Model application

183 The simulation domain, which covers Jiangsu, Zhejiang, Anhui, Shanghai, and neighboring  
184 provinces, has a horizontal resolution of 4 km  $\times$  4 km (238  $\times$  268 grids) and a vertical structure of  
185 18 layers as shown in Fig. S2S1. Details of the domain setup can be found in previous studies (Li  
186 et al., 2021<sup>2022</sup>; Li et al., 2022<sup>2021</sup>). The meteorological field was predicted by the Weather  
187 Research and Forecasting (WRF) model version 4.0 with the ECMWF Reanalysis v5.0 (ERA5)  
188 reanalysis data as ~~the~~ inputs. More details about the WRF configuration ~~were~~<sup>have</sup> been  
189 summarized by Wang et al. (2021)<sup>Wang et al. (2021)</sup>. A spin-up of two days was used to minimize  
190 the influence of initial conditions.

191 Biogenic emissions were generated from the Model for Emissions of Gases and Aerosols  
192 from Nature (MEGAN) version 2.1 (~~Guenther et al., 2012~~)<sup>(Guenther et al., 2012)</sup>. Open biomass  
193 burning emissions were based on the Fire INventory from the National Center for Atmospheric  
194 Research (FINN) (~~Wiedinmyer et al., 2011~~)<sup>(Wiedinmyer et al., 2011)</sup>. Anthropogenic emissions  
195 were generated from the updated 2017 emission inventory for the YRD (~~Cheng et al., 2021~~)<sup>(Cheng</sup>  
196 et al., 2021) and the Multi-resolution Emission Inventory for China (MEIC,  
197 <http://www.meicmodel.org>, last access: 1 June 2023) for the rest of the domain. Currently, there  
198 is ~~no available data to use in more~~<sup>a lack of</sup> localized ~~sources~~<sup>source profiles</sup> in China. ~~The detailed~~  
199 ~~emissions of 1-MN, particularly regarding Nap and 2-MN of different sources. These data~~ were  
200 ~~calculated~~<sup>obtained</sup> from the ~~US~~<sup>U.S.</sup> Environmental Protection Agency's (EPA's)

repository of organic gas and particulate matter (PM) speciation profiles of air pollution sources (SPECIATEv5.2) ~~and along with the source~~ information reported by An et al. (2021)<sup>An et al. (2021)</sup> and Li et al. (2014). ~~See the Relevant details of emission calculations can be found in the~~ Supplement ~~for more details about the calculating process.~~. There ~~were~~<sup>are</sup> two sets of emission data consisting of different Nap and MN emissions ~~in the YRD~~. The emis-orig used the original Nap emissions from the 2017 YRD inventory ~~and as well as~~ the calculated Nap emissions in the rest of the domain and MN emissions ~~in the entire domain~~. We show later that Nap and MN were underestimated ~~in emis-orig~~ and required an adjustment in their emissions to capture the observed concentrations. ~~Therefore, the~~Considering their predominantly anthropogenic origin, their anthropogenic emissions ~~of Nap and MN~~ in the ~~YRD~~entire region from emis-orig were multiplied by 5 and 7, respectively, ~~and unchanged in other regions~~ in the emis-adjust case. All the emission ratios applied in this study are shown in Table S2. According to Fig. ~~S3~~S2, Nap and MN emissions were mainly located in Shanghai, southern Jiangsu, and parts of Zhejiang ~~in the YRD region.~~ After adjustments, the total ~~Nap and MN~~ emission rate ~~over~~of Nap and MN in the YRD region in emis-adjust (~~3.9 kg~~85.0 tons day<sup>-1</sup>) was approximately ~~fourfold~~4 times higher than that in emis-orig (~~0.9 kg~~18.2 tons day<sup>-1</sup>). The total MN emission rate ~~over~~in the YRD region in emis-adjust was ~~0.9 kg~~20.3 tons day<sup>-1</sup> ~~and was~~ lower than that of Nap. For emis-adjust, the dominant source of MN was residential-related (47.0%), followed by industry process (25.8%) and on-road ~~transport~~transportation (20.8%). ~~On~~Among all sources, on-road ~~transport~~transportation contributed the most to Nap emissions in both emis-orig (78.2%) and emis-adjust (87.5%). It should be noted that uncertainties associated with the emission inventory and source profiles, which are based on sector-specific mass ratios presented in Table S2, may potentially affect both

223 the distribution and source contributions of Nap and MN~~may be influenced by the uncertainties~~  
224 ~~in the source profiles.~~

225 Table S3~~1~~ lists the scenarios conducted in this study. In case-1product-orig, the anthropogenic  
226 emissions ~~in the YRD used were based on~~ emis-orig along with ~~default Nap and added MN~~  
227 ~~emissions, and~~ the SOA parameterization for MN ~~was~~ fitted by the one-product method in Fig.  
228 1c and that of Nap fitted by a two-product method in Fig. 1a under high-NO<sub>x</sub> conditions. To assess  
229 the impacts of different SOA parameterizations, ~~the~~ case-2products-orig ~~shared~~adopted the same  
230 setting ~~with~~as case-1product-orig except ~~that a two product method for MN generated~~utilizing a  
231 two-product method for MN-derived SOA ~~was employed. Both~~under high-NO<sub>x</sub> conditions (Fig.  
232 1b). For accurate representations of the fate of Nap and MN in the atmosphere, both case-1product  
233 and case-2products ~~used~~employed adjusted emissions (emis-adjust ~~as the emission inventory but~~)  
234 along with different SOA parameterizations for MN. ~~In~~SOA formation from Nap and MN under  
235 low-NO<sub>x</sub> conditions in the above cases were all characterized by a fixed yield as shown in Table  
236 S1. Overall, the contributions of Nap, 1-MN, and 2-MN to the aromatic SOC were estimated based  
237 on different emission inventories and ~~two~~ SOA ~~parameterization~~-schemes. To evaluate the effects  
238 of Nap, 1-MN, and 2-MN on O<sub>3</sub>, SOC, and radical concentrations, their emissions in case-1product  
239 were set to zero and named ~~base1.~~base\_zeroNapMN. A case named base\_zeroMN was conducted  
240 to quantify the individual effects of Nap and MN by setting the emissions of 1-MN and 2-MN to  
241 zero.

## 242 2.3 Observation data for model validation

243 In May-June 2018, the EXPLORE-YRD field campaign was launched at a rural site in  
244 Taizhou (32.558°N, 119.994°E) and simultaneously monitored VOCs (including Nap and MN),  
245 O<sub>3</sub>, NO<sub>x</sub>, ~~SOC~~, organic carbon (OC), OH~~·~~· hydroperoxy radical (HO<sub>2</sub>·), and other various

246 pollutants, which provides a good opportunity for model validation and understanding the  
247 evolution of air pollution in the YRD (Wang et al., 2020<sup>2020a</sup>; Huang et al., 2020; Yu et al., 2021;  
248 Gao et al., 2022). Details of the measurement method and accuracy for each species refer to these  
249 references. The simulated ~~MDA8 daily maximum 8-hour average (MDA8)~~ O<sub>3</sub>, fine particulate  
250 matter (PM<sub>2.5</sub>), sulfur dioxide (SO<sub>2</sub>), nitrogen dioxide (NO<sub>2</sub>), and carbon monoxide (CO) were  
251 also compared with the observations from the National Real-Time Urban Air Quality Release  
252 Platform of the China Environmental Monitoring Center (<http://106.37.208.233:20035/>, last  
253 access on May 17, 2023) in Suzhou, Nanjing, Hangzhou, Hefei, and Shanghai cities as shown in  
254 Fig. S2. ~~The statistical metries including NMB, NME, and r were calculated for several air~~  
255 ~~pollution species. The model performance benchmarks followed the recommendations by Emery~~  
256 ~~et al. (2017) and are listed in Table S4.~~ S1. ~~The statistical metrics including normalized mean bias~~  
257 ~~(NMB), normalized mean error (NME), and correlation coefficient (r) were calculated for several~~  
258 ~~air pollution species. The benchmarks for model performance followed the recommendations by~~  
259 ~~Emery et al. (2017) and are listed in Table S3.~~ The meteorological parameters predicted by WRF  
260 have been examined to be robust during the same episode by Wang et al. (2021) Wang et al. (2021).

### 261 3 Results

#### 262 3.1 Model validation

263 Fig. 1Figure 2 and Fig. S4S3 show the comparison of observed and simulated hourly  
264 variations of Nap, MN, O<sub>3</sub>, ~~organic carbon (OC)~~ and PM<sub>2.5</sub> at the Taizhou site during the study  
265 period. ~~As shown in Fig. 1, in the original settings, the~~ The concentrations of Nap ~~in case-1 product-~~  
266 ~~orig and case-2 products-orig~~ were ~~largely significantly~~ underestimated ~~in emis-orig~~ by 79%  
267 compared ~~with to~~ the observations, ~~with the value of NMB being 0.79~~. In contrast, emis-adjust  
268 better represented the temporal variations of Nap (NMB=0.01, r=0.68) than emis-orig, with the

269 averaged average concentration increased increasing by 375% a factor of 4 and more comparable  
270 to agreeing well with the observations. The concentrations modeled concentration of MN simulated  
271 by emis-adjust (1.40E-2 ppb) were 14.0 ppt was also comparable to the observations (1.50E-2  
272 ppb observed value (15.0 ppt) and showed a good correlation with between the observations two  
273 (r=0.59). For other species, the concentrations of OC and PM<sub>2.5</sub> were also improved slightly  
274 increased in emis-adjust compared to that of emis-orig, although they were underestimated in both  
275 scenarios. The NMB and NME of PM<sub>2.5</sub> satisfied the benchmark benchmarks recommended by  
276 Emery et al. (2017) Emery et al. (2017), while the NMB of the maximum daily 8-hour average  
277 (MDA8) O<sub>3</sub> exceeded the benchmark criteria. Table S5S4 shows that the concentrations of NO<sub>2</sub>  
278 and nitric oxide (NO) were underestimated at the Taizhou site suggested by the negative NMB  
279 values. The simulated OH radicals compared agreed well with the observation observations while  
280 the concentrations of HO<sub>2</sub>· were underestimated at the Taizhou site (Fig. S5). It should be  
281 noted that the influences of different SOA schemes for MN on the aforementioned species are  
282 negligible. The predicted concentrations of MDA8 O<sub>3</sub>, PM<sub>2.5</sub>, SO<sub>2</sub>, NO<sub>2</sub>, and CO in other cities  
283 were also examined as shown in Table S4. Overall, the model agreed well with observations in  
284 most of the cities except for a significant underestimation of MAD8 O<sub>3</sub> in Shanghai. We chose the  
285 (Table S3). The results from of case-1 product and case-2 products using emis-adjust as the emission  
286 data were superior compared to the cases using emis-orig. These findings will be further discussed  
287 in the subsequent analysis.

### 288 3.2 Influences of Nap and MN on SOC in Taizhou

289 Figure 23 depicts the diurnal variations of emissions and concentrations of Nap, 1-MN, and  
290 2-MN, as well as the corresponding SOC products SOC-Nap, SOC-1MN, and SOC-2MN at the  
291 Taizhou site in both case-1 product and case-2 products. The emissions of Nap, 1-MN, and 2-MN

exhibited a bimodal pattern. For Nap, the bimodal characteristics were the most pronounced, accompanied by two peaks that occurred between 8:00~9:00 and 16:00~17:00, respectively. This was likely attributed to the dominant source of Nap from ~~transport~~transportation as described in Sect. 2.2. Nap and MN concentrations were relatively low during the daytime and peaked in the morning and at night, ~~which was~~. This is caused by the fast photochemical removal and increased dilution during the daytime, along with the facilitated accumulation due to low mixing heights at night (Cohan et al., 2013; Huang et al., 2019; Cohan et al., 2013). The simulated diurnal variation of Nap agreed well with observations, but the daytime MN concentration was underpredicted as shown in Fig. S5. The concentrations of SOC generated by Nap, 1-MN, and 2-MN were high during the daytime, especially from 10:00 to 15:00. This was attributed to the removal of Nap and MN by OH radicals to form SOC. The potential removal by ~~nighttime~~ nitrate radicals ( $\text{NO}_3$ ) was negligible in this study, leading to a ~~certain degree of declining trend for~~decline in SOC formation at night. Nap-derived SOC was the most abundant, followed by SOC from 2-MN (~~SOC-2MN~~) and 1-MN (~~SOC-1MN~~). This is attributed to the combined effects of the  $\text{OH}^\cdot$  reactivity, SOA yields, as well as abundances of the three compounds (Li et al., 2017; Yu et al., 2021). ~~Apart from the highest emissions of Nap, Nap is also more reactive with  $\text{OH}^\cdot$  and has the highest SOA yield in case 2 products compared to the other two species. In case 1 product, although the SOA yields of MN are the highest, the  $\text{OH}^\cdot$  reaction rate with Nap is faster than MN. Apart from having the highest emissions, Nap also exhibits greater reactivity with  $\text{OH}^\cdot$ . Although its SOA yield under high- $\text{NO}_x$  conditions is lower than that of MN fitted by the one-product scheme (Fig. S6), its SOA yield under low- $\text{NO}_x$  conditions is the highest among the three PAHs (Table S1). Overall, Nap contributed the most to SOC. 2-MN demonstrates higher SOA yields than 1-MN under high- $\text{NO}_x$  conditions in both cases, but a lower SOA yield under low- $\text{NO}_x$  conditions. Considering the impact~~

315 of a higher emission rate (Fig. 3a and 3c), 2-MN contributed two times more SOC compared to 1-  
316 MN. The SOC generated by MN in case-2products was lower than that in case-1product due to  
317 the lower SOA yield ~~of MN~~ applied in case-2products ~~as shown in Table S1 (Fig. S6).~~

318 Figure 34 shows the contributions of major aromatic species, i.e., Nap, 1-MN, 2-MN, 1,2,4-  
319 trimethyl benzene (B124), xylene (MPO), benzene (BENZ), toluene (TOLU), aromatics with  $k_{OH}$   
320 (reaction rate constant with  $OH\cdot$ )  $< 2 \times 10^4$  ppm $^{-1}$  min $^{-1}$  (ARO1) and ARO2MN' (ARO2 excluding  
321 Nap and MN) to the total emissions of aromatics and the aromatic-derived SOC in both case-  
322 1product and case-2products at the Taizhou site. Among all the species, ARO2MN', MPO, and  
323 B124 showed the largest fraction ~~of in~~ emissions, accounting for 58.6%, followed by ARO1 and  
324 TOLU (31.8%), and BENZ (6.3%). Nap and MN contributed the least to the total aromatic  
325 emissions, with Nap ~~to be being~~ the most abundant species. The daily average concentrations of  
326 SOC produced from all the aromatics ~~was were~~ quite similar in case-1product and case-2products,  
327 ~~which were 102.0 with the values of 101.3~~ and 100.72 ng m $^{-3}$ , respectively (Fig. S6S7). The  
328 contribution of ARO2MN', MPO, and B124 to the total aromatic-derived SOC was the most  
329 significant, ~~which was ranging from 45.6% to 46.2–45.8%~~. Nap ~~showed indicated~~ a remarkable  
330 contribution to SOC, accounting for 8.7–8.8%, ~~although it 2–8.3%, despite constituting~~ only ~~made~~  
331 ~~up~~ 2.6% of the total emitted aromatics. 2-MN was also an important SOC precursor, contributing  
332 ~~to 1.3–2.2–2.0%~~ of the aromatic-derived SOC. 1-MN ~~was showed~~ the ~~least emitted aromatic~~  
333 ~~compound lowest emissions~~, accounting for 0.2% of the total aromatic emissions and less than 1.0%  
334 of the aromatic-derived SOC. ~~All of Overall~~, Nap, 1-MN, and 2-MN ~~had exhibited~~ the same trait of  
335 contributing ~~much significantly~~ more to SOC than to ~~SOC~~ precursor emissions, especially for Nap.  
336 The total contributions of MN and Nap to SOC were higher than that of BENZ, even though their  
337 emissions were significantly lower than BENZ. Similar results were also found in field campaigns

338 conducted in Guangzhou (Fang et al., 2021) (Fang et al., 2021) and Beijing (Huang et al.,  
339 2019) (Huang et al., 2019) where Nap and MN showed higher contributions. Compared to  
340 BENZbenzene and other single-ring monocyclic aromatics, the oxidation products of Nap and MN  
341 belong to IVOCs with lower saturation vapor pressure, which is are much less volatile and are more  
342 likely to generate SOA through coagulation and absorption efficient at aerosol growth (Gao Wang  
343 et al., 2021; Zhao et al., 2014 2020b). Thus, their considerably higher SOA yields and reactivity  
344 with OH<sup>·</sup> lead to an important contribution to SOA formation. In general, we We found that 3.3%  
345 of aromatic emissions from Nap and derivatives could contribute contributed up to 11.7% 10.9% of  
346 SOC generated from aromatics at the Taizhou site.

### 347 3.3 Regional distributions of Nap and MN and the influences on secondary pollutants

348 In the YRD, the average contribution of Nap to aromatic emissions was 4.1% (Fig. S7), while  
349 the Nap-derived SOC accounted for 94.1% of aromatic emissions and contributed 8.0% and 98.1%  
350 of the total SOC generated by aromatics in case-1 product and case-2 products, respectively. (Fig.  
351 S8). We found extremely high contributions of Nap-derived SOC in areas with high Nap emissions  
352 (Fig. S8), reaching up to 13.7 12.6% in case-2 products. 2-MN constituted contributed 0.6% of the  
353 total aromatic emissions and contributed up to 3.8 2.5% of the aromatic-derived SOC in case-  
354 1 product. Among the three PAHs, 1-MN showed the lowest emissions (about 0.4% of the aromatic  
355 emissions) and contributed minimally to the smallest regional average contribution to SOC (0.64–  
356 0.97%). The SOC derived from MN in case-2 products was approximately 38% lower than that in  
357 case-1 product across the entire YRD region (Fig. S8S9), while minor differences were observed  
358 in O<sub>3</sub> and the total SOC showed minor differences in between the two cases with different SOA  
359 parameterization of MN (Fig. S9S10). In general, the concentrations of SOC produced by the three  
360 PAHs in case-1 product were higher than those in case 2 products, which may minimize the

361 ~~discrepancy between the simulated and observed OC given the existing underestimation of OC at~~  
362 ~~least in Taizhou, as shown in Fig. 1 and Fig. S6. Therefore, we opted for that in case-2 products,~~  
363 ~~exhibiting similar spatial distribution patterns in both cases. We will focus on~~ the results from  
364 case-1 product in the subsequent analysis.

365 ~~The accurate reproduction and quantitative constraints~~Accurate representation of Nap and  
366 MN ~~are sources and sinks in model simulations is~~ crucial for ~~understanding~~comprehending the  
367 atmospheric oxidation capacity ~~in model simulations.~~ The relative differences between  
368 ~~base1~~base zeroNapMN and case-1 product were calculated to evaluate the effects of Nap, 1-MN,  
369 and 2-MN on O<sub>3</sub>, SOC, and radical concentrations. As shown in Fig. 4a~~5a~~, the SOC concentrations  
370 ~~over~~in the YRD ~~region~~ increased by approximately 1.0.9% on average, with the most significant  
371 ~~increase~~change observed in areas with high emissions of Nap and MN, such as Shanghai and  
372 southern Jiangsu Province, reaching up to 1.7%. The impact on O<sub>3</sub> was relatively limited, with a  
373 maximum increase of 0.3%%, primarily attributed to Nap rather than MN (Fig. S11). Similar to  
374 SOC, the spatial distribution of O<sub>3</sub> variations was consistent with that of Nap and MN emissions.  
375 ~~When~~By considering the oxidation of Nap and MN ~~oxidation was considered~~ in the model, HO<sub>2</sub><sup>·</sup>  
376 concentration was enhanced across the domain by up to 1.6% (in Shanghai), likely due to the  
377 production of HO<sub>2</sub><sup>·</sup> through the reaction of Nap and MN with OH<sup>·</sup>. However, the variations in  
378 OH<sup>·</sup> concentration exhibited regional heterogeneity, with a maximum increase of 0.8%(7%) in  
379 Shanghai) and a maximum decrease of 0.3% (in Wenzhou). The areas with elevated OH<sup>·</sup>  
380 coincided with the locations experiencing notable increases in O<sub>3</sub>. As an OH<sup>·</sup> source in the  
381 troposphere, the photolysis of O<sub>3</sub> produces electronically excited O(<sup>1</sup>D) atoms that react with water  
382 molecules to form fresh OH<sup>·</sup> (Qin et al., 2022; Tan et al., 2019; Qin et al., 2022). Moreover, the  
383 areas with elevated OH<sup>·</sup> also exhibited a significant increase in HO<sub>2</sub><sup>·</sup>. HO<sub>2</sub><sup>·</sup> can react with O<sub>3</sub> ~~to~~

384 ~~produce OH<sup>·</sup>, thereby offsetting the OH<sup>·</sup> consumption by Nap and MN oxidations (Zhu et al.,~~  
385 ~~2020), or NO to produce OH<sup>·</sup>, thereby offsetting the OH<sup>·</sup> consumption by Nap and MN oxidation~~  
386 ~~(Zhu et al., 2020). In the areas with decreased OH<sup>·</sup>, the increase~~increases of O<sub>3</sub> and HO<sub>2</sub><sup>·</sup> ~~was not~~  
387 ~~significant~~were insignificant, resulting in ~~fewer newly generated~~a reduced generation of OH<sup>·</sup> to  
388 compensate for the OH<sup>·</sup> consumption by Nap and MN. ~~Similar to O<sub>3</sub>, variations in OH<sup>·</sup> and HO<sub>2</sub><sup>·</sup>~~  
389 were primarily influenced by Nap rather than MN (Fig. S11).

390 To ~~minimize the potential obfuscation of~~avoid obscuring the true magnitude by averaging  
391 over the entire episode ~~average variation, the hourly, daily~~ relative differences of SOC, O<sub>3</sub>, and  
392 radicals at the Shanghai and Suzhou sites, which exhibit significant variations, are ~~depicted~~shown  
393 in Fig. 4b5b and Fig. 4c, ~~respectively~~5c. Overall, the influences of Nap and MN varied daily. At  
394 the Shanghai site, the most pronounced effects ~~of~~on OH<sup>·</sup> and HO<sub>2</sub><sup>·</sup> were observed, with increases  
395 of up to 1.79% and 3.78%, respectively. At the Suzhou site, the maximum daily variations of OH<sup>·</sup>  
396 and HO<sub>2</sub><sup>·</sup> (1.5% and 2.9%) were ~~marginally~~slightly lower than those in Shanghai; ~~whereas,~~  
397 However, the ~~maximum~~ daily ~~variations of~~ SOC and O<sub>3</sub> were elevated by up to 3.0% and 1.1% ~~at~~  
398 ~~the~~in Suzhou ~~site~~, respectively. It was found that both OH<sup>·</sup> and HO<sub>2</sub><sup>·</sup> displayed bimodal variations  
399 at the two sites, with the most pronounced changes of 0.7–1.0% and 1.6–2.2% occurring in the  
400 morning, respectively (Fig. S12). The concentrations of SOC and O<sub>3</sub> were elevated in the daytime,  
401 reaching peak increments of 2.1–2.3% and 0.4–0.5% at noon. Consequently, the influences of Nap  
402 and MN on SOC, O<sub>3</sub>, and the atmospheric oxidation capacity were substantial at the daily scale in  
403 those regions.

#### 404 4 Discussion

405 Our results revealed that the contributions of Nap and MN to the total aromatic emissions  
406 were minimal, which were 5.1% in the YRD and 3.3% at the Taizhou site. However, the SOC

407 produced by Nap and MN ~~constituted 12.1~~accounted for 10.4% of the total aromatic-derived SOC  
408 in this region and ~~11.7~~10.9% at the Taizhou site. Given the overestimation of other aromatic  
409 species in the current model (Table S5S4), the contributions of Nap and MN to aromatic SOC  
410 ~~might~~may be underestimated. ~~Yu et al. (2021)~~Yu et al. (2021) demonstrated an augmented fraction  
411 of SOC derived from a yield method to that using the EC tracer method after the inclusion of Nap  
412 and MN oxidation (from 25.3% to 39.5%) during the same episode at the Taizhou site. That is to  
413 say, Nap and MN ~~contributed~~contribute 35.9% of the total SOC estimated by using the SOA yield  
414 multiplied by the consumption of VOCs, which ~~was~~is higher than the value (~~11.7~~10.9) in this  
415 study. Other field studies have also found significant SOA formation from Nap and MN among  
416 aromatics in the Pearl River Delta region (12.4%) (~~Fang et al., 2021~~)(Fang et al., 2021) and in  
417 Beijing during haze days (10.2±1.3%) (~~Huang et al., 2019~~)(Huang et al., 2019), with relatively  
418 smaller contributions to emissions of aromatics by less than 2% and 7%, respectively. This study  
419 highlights the ~~erucial~~important roles of Nap and MN, which exhibit high SOA  
420 ~~production~~formation potentials with trace amounts emitted into the atmosphere. In addition, the  
421 average concentrations of Nap and MN in this study were ~~27~~25 and ~~9~~7 ppt during summer over  
422 the YRD region (Fig. S8S9), respectively. Previous studies have confirmed that the concentrations  
423 of Nap and MN exhibited a seasonal variation, with maxima in winter and minima in summer,  
424 attributed to the increased heating and cooking activities in households during the cold season  
425 (~~Tang et al., 2020; Huang et al., 2019; Fang et al., 2021; Tang et al., 2020~~). Consequently, the  
426 ambient concentration of Nap and MN, along with the potential SOA production may be more  
427 severe in winter. Cleaner fuel types and household cleaning products are recommended for  
428 vehicular and domestic usage.

429 The ~~urgent demand for enhancing the~~improvement in simulation and assessment of Nap and  
430 MN chemistry is ~~necessitated~~crucial. Firstly, the characterization of Nap and MN from local  
431 sources and additional field observations are indispensable to reduce the disparities between the  
432 modeled and observed Nap and MN concentrations. Secondly, the SOA parameterizations of Nap  
433 and MN, including the enthalpy of vaporization and SOA yields, are derived from limited chamber  
434 experiments and require further validation. Previous studies have reported that the SOA yields  
435 obtained from chamber studies were contingent on OH<sup>·</sup> exposure, NO<sub>x</sub> levels, relative humidity,  
436 and seed particles, which may not represent the actual atmospheric conditions (Yu et al., 2021;  
437 Ling et al., 2022). Thirdly, chlorine radicals (Cl), NO<sub>3</sub> radicals, and O<sub>3</sub> also play an important role  
438 in the atmospheric reactions of Nap and MN ([Wang et al., 2005](#); Cohan et al., 2013; ~~Matthieu et~~  
439 ~~al., 2014~~; Riva et al., 2015; ~~Wang et al., 2005; 2014~~; Aleman, 2006), which were missing in the  
440 current study due to the lack of parameterization.— The formation of gas- and particle-phase  
441 products through reactions between Cl atoms and Nap has been confirmed. For instance,  
442 chloronaphthalene and chloroacenaphthenone have been identified as potential SOA markers for  
443 the Cl-initiated oxidation of Nap in the ambient atmosphere ([Riva et al., 2015](#)).[\(Riva et al., 2015\)](#).  
444 As important sources of Cl atoms, abundant nitryl chloride (ClNO<sub>2</sub>) and molecular chlorine (Cl<sub>2</sub>)  
445 ~~were~~are attributed to sea salt, coal combustion, biomass burning (Le Breton et al., 2018), and  
446 urban-originated ~~transports~~transport (Li et al., 2021; Tham et al., ~~2013~~[2014](#)). Consequently, the  
447 Cl-initiated SOA formation process may be pronounced in specific regions, such as the marine  
448 boundary layer and industrial areas. Using the rate constant of Cl with Nap ((4.22±0.46)×10<sup>-12</sup>)  
449 (~~Matthieu et al., 2014~~)[\(Riva et al., 2014\)](#) and corresponding SOA yields (0.91±0.05) (~~Riva et al.,~~  
450 ~~2015~~), ~~which is approximately~~[\(Riva et al., 2015\)](#), ~~which is up to~~ three times higher than those  
451 determined from OH-initiated oxidation (Chan et al., 2009; Shakya and Griffin, 2010), we

452 estimated the potential SOA formation from the reaction of Nap and Cl atoms via a yield method  
453 (Huang et al., 2019; Yu et al., 2021). ~~Assuming a global average Cl concentration of  $1 \times 10^4$~~   
454 ~~molecules cm<sup>-3</sup> and a tropospheric lifetime of 275 days as determined by Matthieu et al. (2014),~~  
455 ~~SOA generated from Nap initiated by Cl atoms is three times higher than that from the oxidation~~  
456 ~~by OH<sup>·</sup> with a 12 h average daytime concentration of  $2 \times 10^6$  molecules cm<sup>-3</sup> and a tropospheric~~  
457 ~~lifetime of 6 hours. Assuming a 12-h average daytime OH<sup>·</sup> concentration of  $2 \times 10^6$  molecules cm<sup>-3</sup>~~  
458 ~~and a photooxidation age of 6 h, the SOA generated from Nap oxidation by Cl atoms can reach up~~  
459 ~~to 56% of that from the Nap + OH pathway in highly polluted regions with a Cl/ OH ratio greater~~  
460 ~~than 0.8 (Choi et al., 2020)~~. This suggests that the omission of Cl-initiated chemistry in this study  
461 might lead to an underestimation of Nap-derived SOA by approximately ~~75~~<sup>36</sup>%. Given the  
462 underestimation of anthropogenic chlorine emissions in China (~~Li et al., 2021~~; Choi et al., 2020;  
463 [Li et al., 2021](#)), further studies are recommended to estimate chlorine emissions with finer spatial  
464 resolution and the impacts on Nap SOA under atmospherically realistic conditions. Lastly, a  
465 precise depiction of Nap and MN chemistry is crucial for gaining a deeper understanding of the  
466 health implications of these noxious compounds. The health risks associated with inhalation  
467 exposure to outdoor Nap and other PAHs have been assessed by calculating the incremental  
468 lifetime cancer risk (ILCR) values in China and the United States (Han et al., 2020; Zhang et al.,  
469 2016). Nonetheless, there has been no systematic evaluation of the health risks resulting from  
470 exposure to PAH-derived SOA and by-products, despite previous studies verifying the  
471 toxicological impacts (e.g. oxidation potential, OP) of Nap-derived SOA (~~Lima-de-Albuquerque~~  
472 ~~et al., 2021~~; Wang et al., 2018; Tuet et al., 2017a; Tuet et al., 2017b; [Lima de Albuquerque et al.,](#)  
473 [2021](#)). More precise measurements of the OP of ~~the~~ different ~~individual~~ SOA [components](#) are  
474 needed ~~in order~~ to evaluate the overall oxidative potentials of ambient SOA ~~using individual~~

475 ~~intrinsic OP of different types of SOA in conjunction with SOA loadings in models~~. Future studies  
476 are needed to develop rational parameterization schemes for assessing the health risks associated  
477 with Nap- and MN-derived SOA.

## 478 **5 Conclusions**

479 In this study, we investigated the impacts of Nap, 1-MN, and 2-MN oxidation on the  
480 formation of SOC, O<sub>3</sub>, and radicals from May 20 to June 18, 2018, in the YRD using a revised  
481 CMAQ model and explicit emission inventories. The ~~simulating~~ results of case-1 product, using  
482 the adjusted emissions (emis-adjust) and a one-product method ~~to fit~~for fitting MN ~~yields~~SOA,  
483 best ~~reproduced~~captured the observed evolution of Nap (NMB=0.01) and MN (NMB=-0.07) when  
484 compared ~~with~~to the default case (NMB=-0.79 for Nap, NMB=-0.85 for MN). The primary sources  
485 of Nap and MN were transportation and residential-related ~~and thus led to~~sectors, resulting in a  
486 bimodal emission pattern ~~for their emissions. Whereas the Nap and MN~~. The concentrations of  
487 Nap and MN were ~~relatively low~~lowest during the daytime ~~and peaked, peaking~~ in the morning,  
488 ~~the generated~~ and at night. Their SOC ~~peaked in~~concentrations reached the maximum value during  
489 the daytime ~~affected by~~due to the ~~photochemistry~~photooxidation of Nap and MN and ~~the evolution~~  
490 ~~of the~~ boundary layer. ~~All of~~evolution. Nap, 1-MN, and 2-MN ~~had exhibited~~ the same trait of  
491 contributing ~~much~~ more to aromatic-derived SOC than to ~~SOC precursor~~ emissions of aromatic  
492 hydrocarbons, especially for Nap. ~~In general, we found that 3.3% of aromatic emissions from Nap~~  
493 ~~and derivatives could contribute up to 11.7% SOC generated from aromatics at the Taizhou site.~~  
494 The average concentration of Nap ~~concentrations reached 27~~was 25 ppt in the YRD, accounting  
495 for 4.1% and ~~98.1%~~ (up to ~~43.7~~12.6%) of total ~~aromatics~~aromatic emissions and aromatic-derived  
496 SOC, respectively. The concentrations of 1-MN and 2-MN were relatively low, with ~~an~~ average  
497 values of 3 and 6 ppt ~~in the YRD, and~~and 5 ppt, respectively. Together, they contributed ~~3.1~~only

498 2.4% of the aromatic-derived SOC. At the regional scale, the impacts of Nap and MN oxidation  
499 on O<sub>3</sub> and radical concentrations were limited. However, substantial increases still occurred in  
500 areas with high Nap and MN emissions and, which cannot be disregarded. The high SOA  
501 formation potential of Nap and MN and its impact on secondary pollutants  
502 proved in this study implied highlight the significance importance of such considering these IVOCs  
503 except for alongside traditional VOCs when implementing air pollution control policies, energy  
504 use strategies, and health risks evaluation.

505

## 506 **Code and data availability**

507 The codes used for all the analyses are available on reasonable request to the corresponding author.  
508 All data used in this research are freely available and may be downloaded from the links and cited  
509 references given in the methods section.

## 510 **Author contributions**

511 F.Y., J.L., and J.H. designed the research and conducted the simulations. Y.G., H.W., S.G., and  
512 K.L. collected the observed data. J.A. and C.H. provided emission data. F.Y. led data  
513 analysis and drafted the main text. J.L., J.H., and M.Q. analyzed the data. All authors  
514 discussed contributed to interpreting the results. F.Y. prepared the manuscript and all authors  
515 helped improve and editing the manuscript.

## 516 **Competing interests**

517 The authors declare no competing interests.

## 518 **Disclaimer**

519 Publisher's note: Copernicus Publications remains neutral with regard to jurisdictional claims  
520 made in the text, published maps, institutional affiliations, or any other geographical representation  
521 in this paper. While Copernicus Publications makes every effort to include appropriate place  
522 names, the final responsibility lies with the authors.

523 **Acknowledgements**

524 This work was financially supported by the National Key R&D Program of China  
525 (2022YFE0136200) and the National Natural Science Foundation of China (No. 42077199).

526 **References**

527 Aleman, G.: The kinetics and mechanisms of chlorine atom reactions with alkylbenzenes and  
528 alkynaphthalenes, *M.S.*, California State University, Fullerton., [148 pp.](#), 2006.  
529 An, J., Huang, C., Huang, D., Qin, M., Liu, H., Yan, R., Qiao, L., Zhou, M., Li, Y., Zhu, S., Wang,  
530 Q., and Wang, H.: Sources of organic aerosols in eastern China: a modeling study with high-  
531 resolution intermediate-volatility and semivolatile organic compound emissions, *Atmos. Chem. Chem.*  
532 Phys., 23, 323-344, [10.5194/acp-23-323-2023](#), 2023.  
533 An, J., Huang, Y., Huang, C., Wang, X., Yan, R., Wang, Q., Wang, H., Jing, S. a., Zhang, Y., Liu,  
534 Y., Chen, Y., Xu, C., Qiao, L., Zhou, M., Zhu, S., Hu, Q., Lu, J., and Chen, C.: Emission inventory  
535 of air pollutants and chemical speciation for specific anthropogenic sources based on local  
536 measurements in the Yangtze River Delta region, China, *Atmospheric Chemistry and*  
537 *Physics*, [Atmos. Chem. Phys.](#), 21, 2003-2025, [10.5194/acp-21-2003-2021](#), 2021.  
538 Chan, A. W. H., Kautzman, K. E., Chhabra, P. S., Surratt, J. D., Chan, M. N., Crouse, J. D., Kürten,  
539 A., Wennberg, P. O., Flagan, R. C., and Seinfeld, J. H.: Secondary organic aerosol formation from  
540 photooxidation of naphthalene and alkynaphthalenes: implications for oxidation of intermediate  
541 volatility organic compounds (IVOCs), *Atmos. Chem. Phys.*, 9, 3049-3060, [10.5194/acp-9-3049-2009](#),  
542 2009.  
543 Chen, C.-L., Kacarab, M., Tang, P., and Cocker, D. R.: SOA formation from naphthalene, 1-  
544 methylnaphthalene, and 2-methylnaphthalene photooxidation, *Atmospheric Environment*, [Atmos.](#)  
545 *Environ.*, 131, 424-433, [10.1016/j.atmosenv.2016.02.007](#), 2016.  
546 Cheng, Y., Yu, Q.-q., Liu, J.-m., Du, Z.-Y., Liang, L.-l., Geng, G.-n., Zheng, B., Ma, W.-l., Qi, H.,  
547 Zhang, Q., and He, K.-b.: Strong biomass burning contribution to ambient aerosol during heating  
548 season in a megacity in Northeast China: Effectiveness of agricultural fire bans?, *Science of The Sci.*  
549 Total *Environment*, [Environ.](#), 754, [10.1016/j.scitotenv.2020.142144](#), 2021.  
550 <https://doi.org/10.1016/j.scitotenv.2020.142144>, 2021.  
551 Choi, M. S., Qiu, X., Zhang, J., Wang, S., Li, X., Sun, Y., Chen, J., and Ying, Q.: Study of  
552 Secondary Organic Aerosol Formation from Chlorine Radical-Initiated Oxidation of Volatile  
553 Organic Compounds in a Polluted Atmosphere Using a 3D Chemical Transport Model,  
554 *Environmental Science & Technology*, [Environ. Sci. Technol.](#), 54, 13409-13418,  
555 10.1021/acs.est.0c02958, 2020.  
556 Cohan, A., Eiguren-Fernandez, A., [Miguel, A. H. J. I. J. o. E.](#), and [Dabub, D.](#): *Pollution*: Secondary

557 organic aerosol formation from naphthalene roadway emissions in the South Coast Air Basin of  
558 California, *International Journal of Environment and Pollution*, 52, 206-224,  
559 [10.1504/IJEP.2013.058461](https://doi.org/10.1504/IJEP.2013.058461) *Int. J. Environ. Pollut.*, 52, 206-224, 2013.

560 Emery, C., Liu, Z., Russell, A. G., Odman, M. T., Yarwood, G., and Kumar, N.: Recommendations  
561 on statistics and benchmarks to assess photochemical model performance, *J. Air Waste  
562 Manage.* Assoc., 67, 582-598, 10.1080/10962247.2016.1265027, 2017.

563 Fang, H., Luo, S., Huang, X., Fu, X., Xiao, S., Zeng, J., Wang, J., Zhang, Y., and Wang, X.:  
564 Ambient naphthalene and methylnaphthalenes observed at an urban site in the Pearl River Delta  
565 region: Sources and contributions to secondary organic aerosol, *Atmospheric Environment*, [Atmos.  
566 Environ.](https://doi.org/10.1016/j.atmosenv.2021.118295), 252, 10.1016/j.atmosenv.2021.118295, 2021.

567 ~~Gao, Y., Li, M., Wan, X., Zhao, X., Wu, Y., Liu, X., and Li, X.: Important contributions of alkenes  
568 and aromatics to VOCs emissions, chemistry and secondary pollutants formation at an industrial  
569 site of central eastern China, *Atmospheric Environment*, 244, 10.1016/j.atmosenv.2020.117927,  
570 2021.~~

571 Gao, Y., Wang, H., Liu, Y., Zhang, X., Jing, S., Peng, Y., Huang, D., Li, X., Chen, S., Lou, S., Li,  
572 Y., and Huang, C.: Unexpected High Contribution of Residential Biomass Burning to Non-  
573 Methane Organic Gases (NMOGs) in the Yangtze River Delta Region of China, *Journal of  
574 Geophysical Research: Atmospheres*, [J. Geophys. Res.-Atmos.](https://doi.org/10.1029/2021jd035050), 127, 10.1029/2021jd035050, 2022.

575 Guenther, A. B., Jiang, X., Heald, C. L., Sakulyanontvittaya, T., Duhl, T., Emmons, L. K., and  
576 Wang, X., *J. G. M. D.*: The Model of Emissions of Gases and Aerosols from Nature version 2.1  
577 (MEGAN2.1): an extended and updated framework for modeling biogenic emissions, *Geosci.  
578 Model Dev.*, 5, 1471-1492, [10.5194/gmd-5-1471-2012](https://doi.org/10.5194/gmd-5-1471-2012), 2012.

579 Han, F., Guo, H., Hu, J., Zhang, J., Ying, Q., and Zhang, H.: Sources and health risks of ambient  
580 polycyclic aromatic hydrocarbons in China, *Sci Total Environ.*, 698, 134229,  
581 10.1016/j.scitotenv.2019.134229, 2020.

582 Hayes, P. L., Carlton, A. G., Baker, K. R., Ahmadov, R., Washenfelder, R. A., Alvarez, S.,  
583 Rappenglück, B., Gilman, J. B., Kuster, W. C., de Gouw, J. A., Zotter, P., Prévôt, A. S. H., Szidat,  
584 S., Kleindienst, T. E., Offenberg, J. H., Ma, P. K., and Jimenez, J. L.: Modeling the formation and  
585 aging of secondary organic aerosols in Los Angeles during CalNex 2010, *Atmospheric Chemistry  
586 and Physics*, [Atmos. Chem. Phys.](https://doi.org/10.5194/acp-15-5773-2015), 15, 5773-5801, 10.5194/acp-15-5773-2015, 2015.

587 Hu, W., Zhou, H., Chen, W., Ye, Y., Pan, T., Wang, Y., Song, W., Zhang, H., Deng, W., Zhu, M.,  
588 Wang, C., Wu, C., Ye, C., Wang, Z., Yuan, B., Huang, S., Shao, M., Peng, Z., Day, D. A.,  
589 Campuzano-Jost, P., Lambe, A. T., Worsnop, D. R., Jimenez, J. L., and Wang, X.: Oxidation Flow  
590 Reactor Results in a Chinese Megacity Emphasize the Important Contribution of S/IVOCs to  
591 Ambient SOA Formation, *Environ. Sci. Technol.*, 56, 6880-6893, 10.1021/acs.est.1c03155, 2022.

592 Huang, D. D., Kong, L., Gao, J., Lou, S., Qiao, L., Zhou, M., Ma, Y., Zhu, S., Wang, H., Chen, S.,  
593 Zeng, L., and Huang, C.: Insights into the formation and properties of secondary organic aerosol  
594 at a background site in Yangtze River Delta region of China: Aqueous-phase processing vs.  
595 photochemical oxidation, *Atmospheric Environment*, [Atmos. Environ.](https://doi.org/10.1016/j.atmosenv.2020.117716), 239, 117716,  
596 <https://doi.org/10.1016/j.atmosenv.2020.117716>, 2020.

597 Huang, G., Liu, Y., Shao, M., Li, Y., Chen, Q., Zheng, Y., Wu, Z., Liu, Y., Wu, Y., Hu, M., Li, X.,  
598 Lu, S., Wang, C., Liu, J., Zheng, M., and Zhu, T.: Potentially Important Contribution of Gas-Phase  
599 Oxidation of Naphthalene and Methylnaphthalene to Secondary Organic Aerosol during Haze  
600 Events in Beijing, *Environ. Sci. Technol.*, 53, 1235-1244, 10.1021/acs.est.8b04523, 2019.

601 Le Breton, M., Hallquist, Å. M., Pathak, R. K., Simpson, D., Wang, Y., Johansson, J., Zheng, J.,  
602 Yang, Y., Shang, D., Wang, H., Liu, Q., Chan, C., Wang, T., Bannan, T. J., Priestley, M., Percival,

603 C. J., Shallcross, D. E., Lu, K., Guo, S., Hu, M., and Hallquist, M.: Chlorine oxidation of VOCs at  
604 a semi-rural site in Beijing: significant chlorine liberation from ClNO<sub>2</sub> and subsequent gas- and  
605 particle-phase Cl–VOC production, *Atmos. Chem. Phys.*, 18, 13013-13030, 10.5194/acp-18-  
606 13013-2018, 2018.

607 Li, J., Zhang, M., Wu, F., Sun, Y., and Tang, G.: Assessment of the impacts of aromatic VOC  
608 emissions and yields of SOA on SOA concentrations with the air quality model RAMS-CMAQ,  
609 *Atmospheric Environment*, *Atmos. Environ.*, 158, 105-115, 10.1016/j.atmosenv.2017.03.035,  
610 2017.

611 Li, J., Zhang, N., Wang, P., Choi, M., Ying, Q., Guo, S., Lu, K., Qiu, X., Wang, S., Hu, M., Zhang,  
612 Y., and Hu, J.: Impacts of chlorine chemistry and anthropogenic emissions on secondary pollutants  
613 in the Yangtze river delta region, *Environmental Pollution*, *Environ. Pollut.* 287, 117624,  
614 <https://doi.org/10.1016/j.envpol.2021.117624>, 2021.

615 Li, L., Xie, F., Li, J., Gong, K., Xie, X., Qin, Y., Qin, M., and Hu, J.: Diagnostic analysis of regional  
616 ozone pollution in Yangtze River Delta, China: A case study in summer 2020, *Sci. Total Environ.*,  
617 812, 151511, 10.1016/j.scitotenv.2021.151511, 2022.

618 Li, M., Zhang, Q., Streets, D. G., He, K. B., Cheng, Y. F., Emmons, L. K., Huo, H., Kang, S. C.,  
619 Lu, Z., Shao, M., Su, H., Yu, X., and Zhang, Y.: Mapping Asian anthropogenic emissions of non-  
620 methane volatile organic compounds to multiple chemical mechanisms, *Atmos. Chem. Phys.*, 14,  
621 5617-5638, 10.5194/acp-14-5617-2014, 2014.

622 Lima de Albuquerque, Y., Berger, E., Tomaz, S., George, C., and *Géloën*, A.: Evaluation of  
623 the Toxicity on Lung Cells of By-Products Present in Naphthalene Secondary Organic Aerosols,  
624 *Life (Basel)*, 11, [10.3390/life11040319](https://doi.org/10.3390/life11040319), 2021.

625 Ling, Z., Wu, L., Wang, Y., Shao, M., Wang, X., and Huang, W.: Roles of semivolatile and  
626 intermediate-volatility organic compounds in secondary organic aerosol formation and its  
627 implication: A review, *J. Environ. Sci. (China)*, 114, 259-285, 10.1016/j.jes.2021.08.055, 2022.

628 Liu, T., Wang, X., Deng, W., Hu, Q., Ding, X., Zhang, Y., He, Q., Zhang, Z., Lü, S., Bi, X., Chen,  
629 J., and Yu, J.: Secondary organic aerosol formation from photochemical aging of light-duty  
630 gasoline vehicle exhausts in a smog chamber, *Atmospheric Chemistry and Physics*, *Atmos. Chem.  
631 Phys.*, 15, 9049-9062, 10.5194/acp-15-9049-2015, 2015.

632 Majdi, M., Sartelet, K., Lanzafame, G. M., Couvidat, F., Kim, Y., Chrit, M., and Turquety, S.:  
633 Precursors and formation of secondary organic aerosols from wildfires in the Euro-Mediterranean  
634 region, *Atmospheric Chemistry and Physics*, *Atmos. Chem. Phys.*, 19, 5543-5569, 10.5194/acp-  
635 19-5543-2019, 2019.

636 *Matthieu, Riva, Robert, M., Healy, Pierre Marie, Flaud, Emilie, Perraudin, and A, J. J. J. o. P. C.:  
637 Kinetics of the Gas Phase Reactions of Chlorine Atoms with Naphthalene, Acenaphthene, and  
638 Acenaphthylene, 2014.*

639 Pye, H. O. and Pouliot, G. A.: Modeling the role of alkanes, polycyclic aromatic hydrocarbons,  
640 and their oligomers in secondary organic aerosol formation, *Environ. Sci. Technol.*, 46, 6041-  
641 6047, 10.1021/es300409w, 2012.

642 Pye, H. O. T. and Seinfeld, J. H.: A global perspective on aerosol from low-volatility organic  
643 compounds, *Atmospheric Chemistry and Physics*, *Atmos. Chem. Phys.*, 10, 4377-4401,  
644 10.5194/acp-10-4377-2010, 2010.

645 Qin, M., Hu, A., Mao, J., Li, X., Sheng, L., Sun, J., Li, J., Wang, X., Zhang, Y., and Hu, J.:  
646 *PM<sub>2.5</sub>* and *O<sub>3</sub>* relationships affected by the atmospheric oxidizing capacity in the  
647 Yangtze River Delta, China, *Sci. Total Environ.*, 810, 152268,  
648 <https://doi.org/10.1016/j.scitotenv.2021.152268>, 2022.

649 Riva, M., Healy, R. M., Flaud, P.-M., Perraudin, E., Wenger, J. C., and Villenave, E.: [Kinetics of](#)  
650 [the Gas-Phase Reactions of Chlorine Atoms with Naphthalene, Acenaphthene, and](#)  
651 [Acenaphthylene, J. Phys. Chem. A, 118, 3535-3540, 10.1021/jp5009434, 2014.](#)

652 Riva, M., Healy, R. M., Flaud, P.-M., Perraudin, E., Wenger, J. C., and Villenave, E.: Gas-  
653 and Particle-Phase Products from the Chlorine-Initiated Oxidation of Polycyclic Aromatic  
654 Hydrocarbons, [J. Phys. Chem. A, 119, 11170-11181, 10.1021/acs.jpca.5b04610, 2015.](#)

655 Robinson, A. L., Donahue, N. M., Shrivastava, M. K., Weitkamp, E. A., Sage, A. M., Grieshop, A.  
656 P., Lane, T. E., Pierce, J. R., and Pandis, S. N.: Rethinking organic aerosols: semivolatile emissions  
657 and photochemical aging, [Science, 315, 1259-1262, 10.1126/science.1133061, 2007.](#)

658 Shakya, K. M. and Griffin, R. J.: Secondary Organic Aerosol from Photooxidation of Polycyclic  
659 Aromatic Hydrocarbons, [Environmental Science & Technology, Environ. Sci. Technol., 44, 8134-](#)  
660 [8139, 10.1021/es1019417, 2010.](#)

661 Tan, Z., Lu, K., Hofzumahaus, A., Fuchs, H., Bohn, B., Holland, F., Liu, Y., Rohrer, F., Shao, M.,  
662 Sun, K., Wu, Y., Zeng, L., Zhang, Y., Zou, Q., Kiendler-Scharr, A., Wahner, A., and Zhang, Y.:  
663 Experimental budgets of OH,  $\text{HO} <sub>2</sub>$ , and  $\text{HO}_2$ , and  
664  $\text{RO} <sub>2</sub>$  radicals and implications for ozone formation in the Pearl River  
665 Delta in China 2014, [Atmospheric Chemistry and Physics, Atmos. Chem. Phys., 19, 7129-7150,](#)  
666 [10.5194/acp-19-7129-2019, 2019.](#)

667 Tang, T., Cheng, Z., Xu, B., Zhang, B., Zhu, S., Cheng, H., Li, J., Chen, Y., and Zhang, G.: Triple  
668 Isotopes ( $\delta^{13}\text{C}$ ,  $\delta^{2}\text{H}$ , and  $\Delta^{14}\text{C}$ ) Compositions and Source Apportionment of Atmospheric  
669 Naphthalene: A Key Surrogate of Intermediate-Volatility Organic Compounds (IVOCs),  
670 [Environmental Science & Technology, Environ. Sci. Technol., 54, 5409-5418,](#)  
671 [10.1021/acs.est.0c00075, 2020.](#)

672 Tham, Y. J., Yan, C., Xue, L., Zha, Q., Wang, X., and Wang, T. J. C. S. B.: Presence of high nitril  
673 chloride in Asian coastal environment and its impact on atmospheric photochemistry, [2013 Chin.](#)  
674 [Sci. Bull., 59, 356-359, 10.1007/s11434-013-0063-y, 2014.](#)

675 Tuet, W. Y., Chen, Y., Fok, S., Gao, D., Weber, R. J., Champion, J. A., and Ng, N. L.: Chemical  
676 and cellular oxidant production induced by naphthalene secondary organic aerosol (SOA): effect  
677 of redox-active metals and photochemical aging, [Sci. Rep., 7, 15157, 10.1038/s41598-017-15071-](#)  
678 [8, 2017a.](#)

679 Tuet, W. Y., Chen, Y., Xu, L., Fok, S., Gao, D., Weber, R. J., and Ng, N. L.: Chemical oxidative  
680 potential of secondary organic aerosol (SOA) generated from the photooxidation of biogenic and  
681 anthropogenic volatile organic compounds, [Atmospheric Chemistry and Physics, Atmos. Chem.](#)  
682 [Phys., 17, 839-853, 10.5194/acp-17-839-2017, 2017b.](#)

683 Wang, H., Chen, X., Lu, K., Hu, R., Li, Z., Wang, H., Ma, X., Yang, X., Chen, S., Dong, H., Liu,  
684 Y., Fang, X., Zeng, L., Hu, M., and Zhang, Y.: NO<sub>3</sub> and N<sub>2</sub>O<sub>5</sub> chemistry at a suburban site during  
685 the EXPLORE-YRD campaign in 2018, [Atmospheric Environment, Atmos. Environ., 224,](#)  
686 [10.1016/j.atmosenv.2019.117180, 2020a.](#)

687 Wang, L., Arey, J., and Atkinson, R.: Reactions of Chlorine Atoms with a Series of Aromatic  
688 Hydrocarbons, [Environmental Science & Technology, Environ. Sci. Technol., 39, 5302-5310,](#)  
689 [10.1021/es0479437, 2005.](#)

690 [Wang, M., Chen, D., Xiao, M., Ye, Q., Stolzenburg, D., Hofbauer, V., Ye, P., Vogel, A. L., Mauldin,](#)  
691 [R. L., Amorim, A., Baccarini, A., Baumgartner, B., Brilke, S., Dada, L., Dias, A., Duplissy, J.,](#)  
692 [Finkenzeller, H., Garmash, O., He, X.-C., Hoyle, C. R., Kim, C., Kvashnin, A., Lehtipalo, K.,](#)  
693 [Fischer, L., Molteni, U., Petäjä, T., Pospisilova, V., Quéléver, L. L. J., Rissanen, M., Simon, M.,](#)  
694 [Tauber, C., Tomé, A., Wagner, A. C., Weitz, L., Volkamer, R., Winkler, P. M., Kirkby, J., Worsnop,](#)

695 [D. R., Kulmala, M., Baltensperger, U., Dommen, J., El-Haddad, I., and Donahue, N. M.: Photo-](#)  
696 [oxidation of Aromatic Hydrocarbons Produces Low-Volatility Organic Compounds, Environ. Sci.](#)  
697 [Technol., 54, 7911-7921, 10.1021/acs.est.0c02100, 2020b.](#)

698 Wang, S., Ye, J., Soong, R., Wu, B., Yu, L., Simpson, A. J., and Chan, A. W. H.: Relationship  
699 between chemical composition and oxidative potential of secondary organic aerosol from  
700 polycyclic aromatic hydrocarbons, [Atmospheric Chemistry and Physics, Atmos. Chem. Phys.](#), 18,  
701 3987-4003, 10.5194/acp-18-3987-2018, 2018.

702 Wang, X., Li, L., Gong, K., Mao, J., Hu, J., Li, J., Liu, Z., Liao, H., Qiu, W., Yu, Y., Dong, H., Guo,  
703 S., Hu, M., Zeng, L., and Zhang, Y.: Modelling air quality during the EXPLORE-YRD campaign  
704 – Part I. Model performance evaluation and impacts of meteorological inputs and grid resolutions,  
705 [Atmospheric Environment, Atmos. Environ.](#), 246, 10.1016/j.atmosenv.2020.118131, 2021.

706 Wiedinmyer, C., Akagi, S. K., Yokelson, R. J., Emmons, L. K., Al-Saadi, J. A., Orlando, J. J., and  
707 Soja, A. J.: The Fire INventory from NCAR (FINN): a high resolution global model to estimate  
708 the emissions from open burning, [Geosci. Model Dev.](#), 4, 625-641, 10.5194/gmd-4-625-2011,  
709 2011.

710 Yu, Y., Wang, H., Wang, T., Song, K., Tan, T., Wan, Z., Gao, Y., Dong, H., Chen, S., Zeng, L., Hu,  
711 M., Wang, H., Lou, S., Zhu, W., and Guo, S.: Elucidating the importance of semi-volatile organic  
712 compounds to secondary organic aerosol formation at a regional site during the EXPLORE-YRD  
713 campaign, [Atmospheric Environment, Atmos. Environ.](#), 246, 10.1016/j.atmosenv.2020.118043,  
714 2021.

715 Zhang, H. and Ying, Q.: Secondary organic aerosol formation and source apportionment in  
716 Southeast Texas, [Atmospheric Environment, Atmos. Environ.](#), 45, 3217-3227,  
717 10.1016/j.atmosenv.2011.03.046, 2011.

718 Zhang, H. and Ying, Q.: Secondary organic aerosol from polycyclic aromatic hydrocarbons in  
719 Southeast Texas, [Atmospheric environment, Atmos. Environ.](#), 55, 279-287, 2012.

720 Zhang, J., Wang, P., Li, J., Mendola, P., Sherman, S., and Ying, Q.: Estimating population exposure  
721 to ambient polycyclic aromatic hydrocarbon in the United States - Part II: Source apportionment  
722 and cancer risk assessment, [Environ. Int.](#), 97, 163-170, 10.1016/j.envint.2016.08.024, 2016.

723 Zhang, Y. and Tao, S.: Global atmospheric emission inventory of polycyclic aromatic  
724 hydrocarbons (PAHs) for 2004, [Atmospheric Environment, Atmos. Environ.](#), 43, 812-819,  
725 10.1016/j.atmosenv.2008.10.050, 2009.

726 [Zhao, Y., Hennigan, C. J., May, A. A., Tkacik, D. S., de Gouw, J. A., Gilman, J. B., Kuster, W. C.,](#)  
727 [Berbon, A., and Robinson, A. L.: Intermediate Volatility Organic Compounds: A Large Source of](#)  
728 [Secondary Organic Aerosol, Environmental Science & Technology, 48, 13743-13750,](#)  
729 [10.1021/es5035188, 2014.](#)

730 Zhu, J., Wang, S., Wang, H., Jing, S., Lou, S., Saiz-Lopez, A., and Zhou, B.: Observationally  
731 constrained modeling of atmospheric oxidation capacity and photochemical reactivity in Shanghai,  
732 China, [Atmospheric Chemistry and Physics, Atmos. Chem. Phys.](#), 20, 1217-1232, 10.5194/acp-20-  
733 1217-2020, 2020.

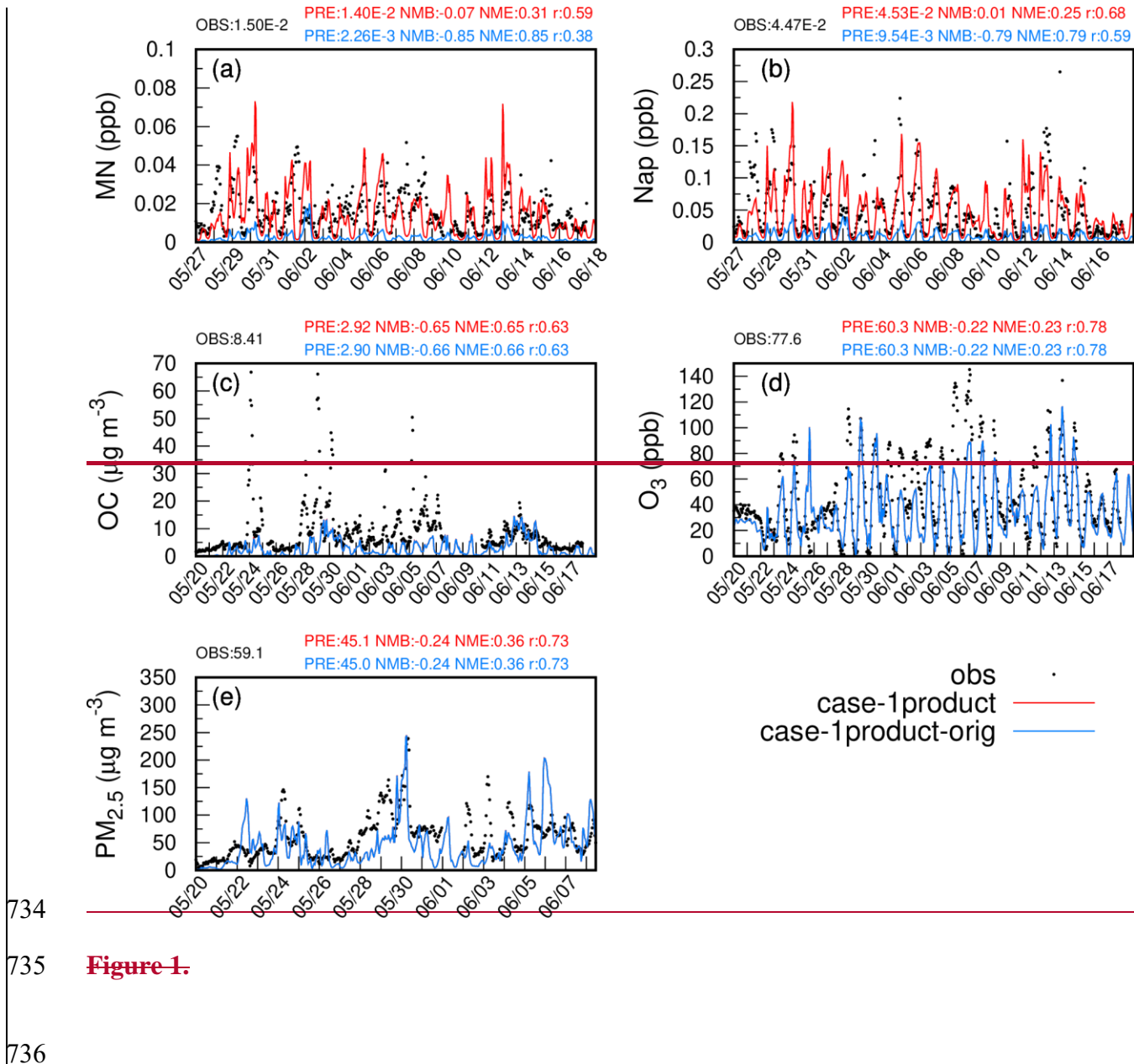
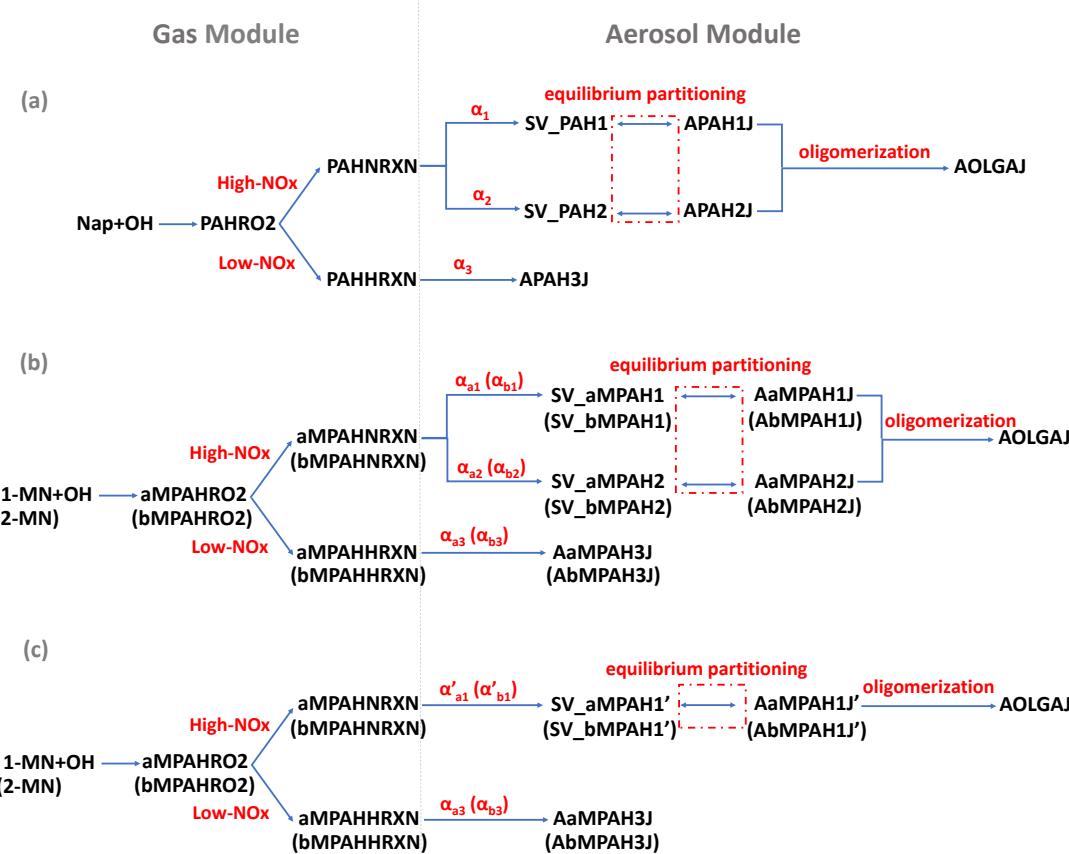


Figure 1.

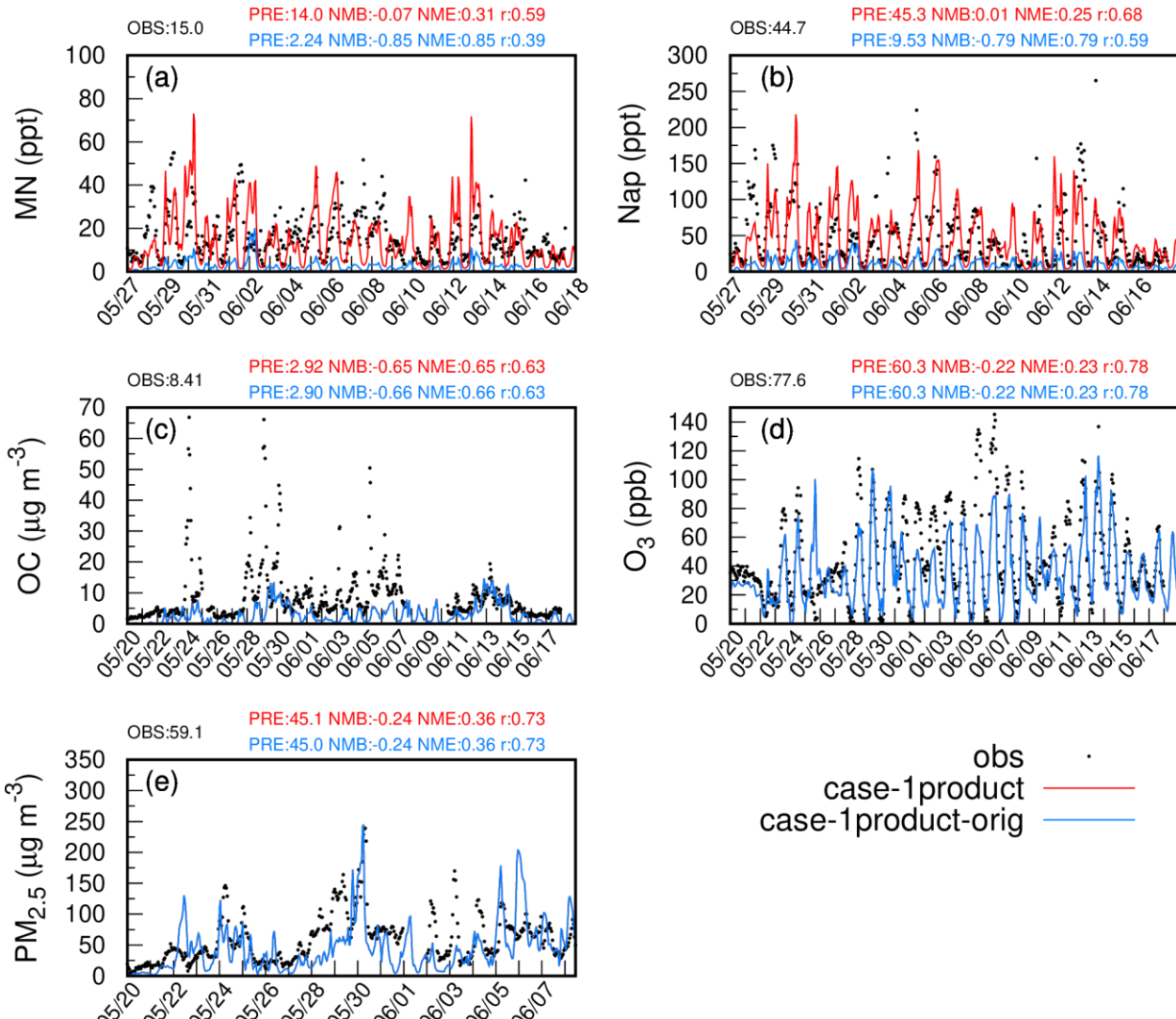
**Table 1.** Settings of the scenarios.

<u>Case</u>	<u>Emission setting</u>	<u>parameterization</u> <u>for MN</u>
<u>case-1product-orig</u>	<u>Nap emissions in the YRD were based on the 2017 YRD inventory; Nap emissions in the rest of the domain and MN emissions in the entire domain were calculated using sector-specific mass ratios and total emissions of non-methane volatile organic compounds (emis-orig)</u>	<u>one-product method</u>
<u>case-2products-orig</u>		<u>two-product method</u>
<u>case-1product</u>	<u>The anthropogenic emissions of Nap and MN in the entire domain from emis-orig were multiplied by 5 and 7, respectively (emis-adjust)</u>	<u>one-product method</u>
<u>case-2products</u>		<u>two-product method</u>
<u>base_zeroNapMN</u>	<u>Emissions of Nap and MN were set to zero based on emis-adjust</u>	<u>one-product method</u>
<u>base_zeroMN</u>	<u>Emissions of MN were set to zero based on emis-adjust</u>	<u>one-product method</u>

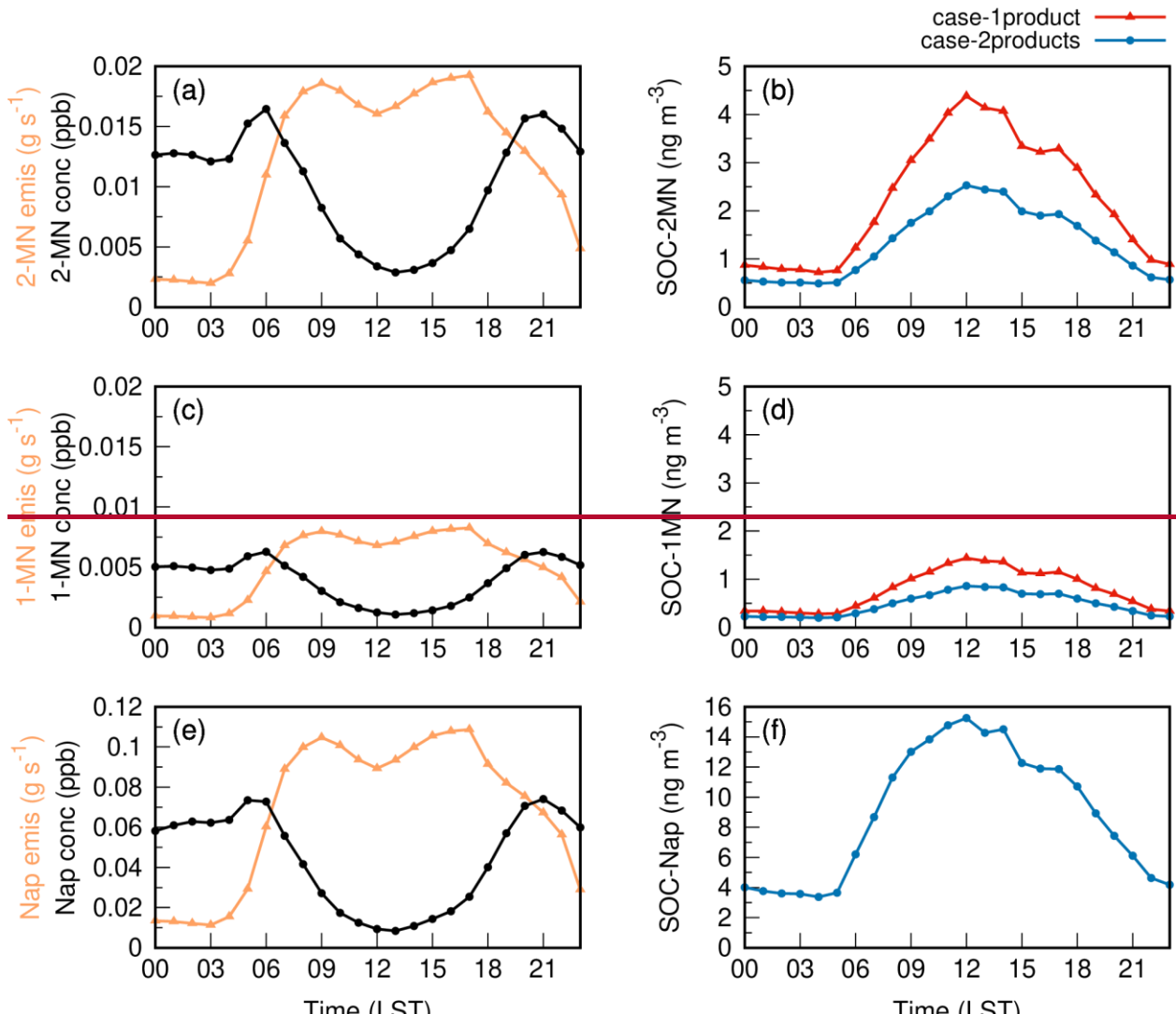


739  
740  
741  
742  
743  
744  
745  
746  
747

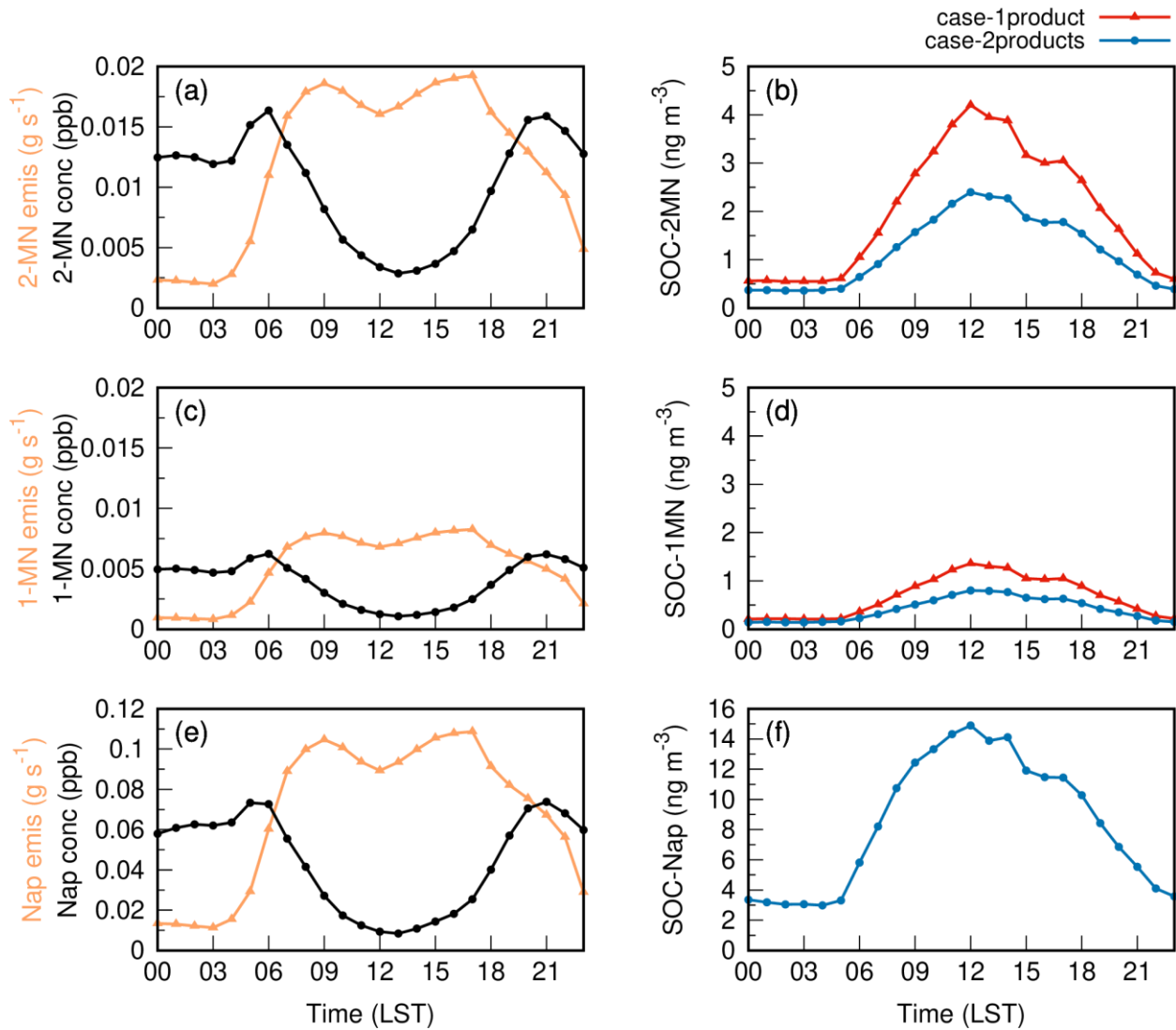
**Figure 1.** SOA schemes for naphthalene (Nap), 1-methylnaphthalene (1-MN), and 2-methylnaphthalene (2-MN) in the updated CMAQ model. (a) pre-existing Nap-derived SOA formation pathways fitted by two products under high NO<sub>x</sub>; (b) newly added SOA formation pathways for 1-MN and 2-MN fitted by two products under high NO<sub>x</sub>; (c) newly added SOA formation pathways for 1-MN and 2-MN fitted by one product under high NO<sub>x</sub>. SOA formation from Nap and MN oxidation by OH radicals under low-NO<sub>x</sub> conditions is represented by a fixed yield. Parameters for 2-MN are indicated in brackets in (b) and (c). The values of  $\alpha$  refer to Table S1.



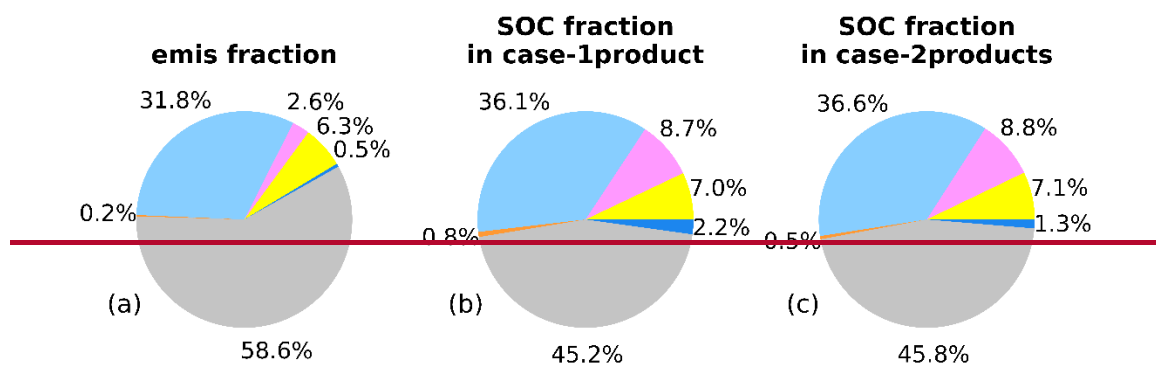
748 **Figure 2.** Observed and simulated hourly concentrations of MN, Nap, OC, PM<sub>2.5</sub>, and O<sub>3</sub> based  
 749 on emis-adjust (red) and emis-orig (blue) at the Taizhou site. Model performances ~~off~~for daily MN,  
 750 Nap, OC, PM<sub>2.5</sub>, and MDA8 O<sub>3</sub> are shown in blue for case-1product-orig and in red for case-  
 751 1product. OBS and PRE represent ~~averaged concentrations~~the average of observations and  
 752 predictions, respectively. Note that the red and blue lines overlap in (c)-(e).



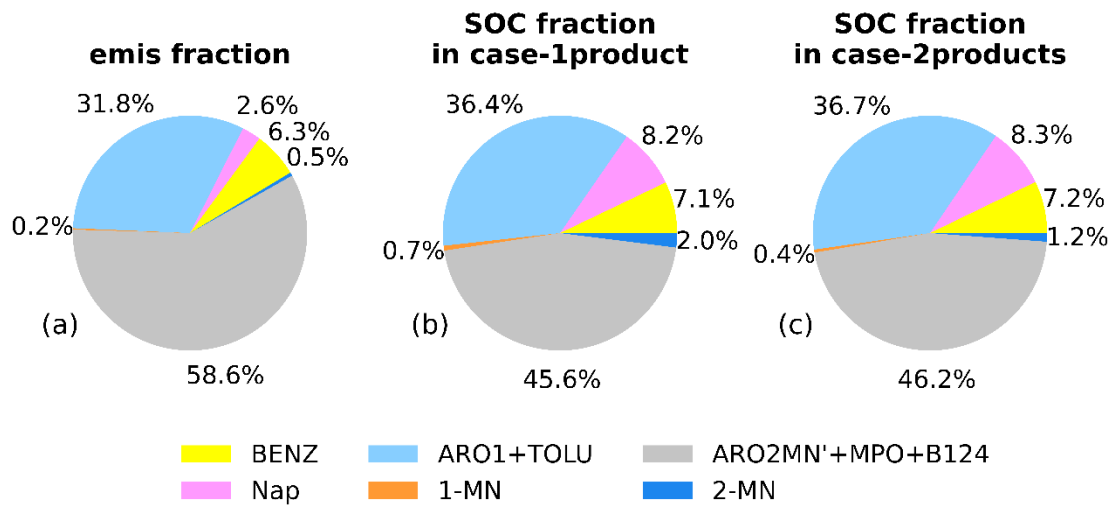
754  
755



756  
757 **Figure 23.** Diurnal variations of emissions (yellow line) and predicted concentrations (black line)  
758 for 2-MN (a), 1-MN (c), and Nap (e), as well as the corresponding SOC concentrations (b, d, f) at  
759 the Taizhou site. [Note that the red and blue lines overlap in \(f\).](#)

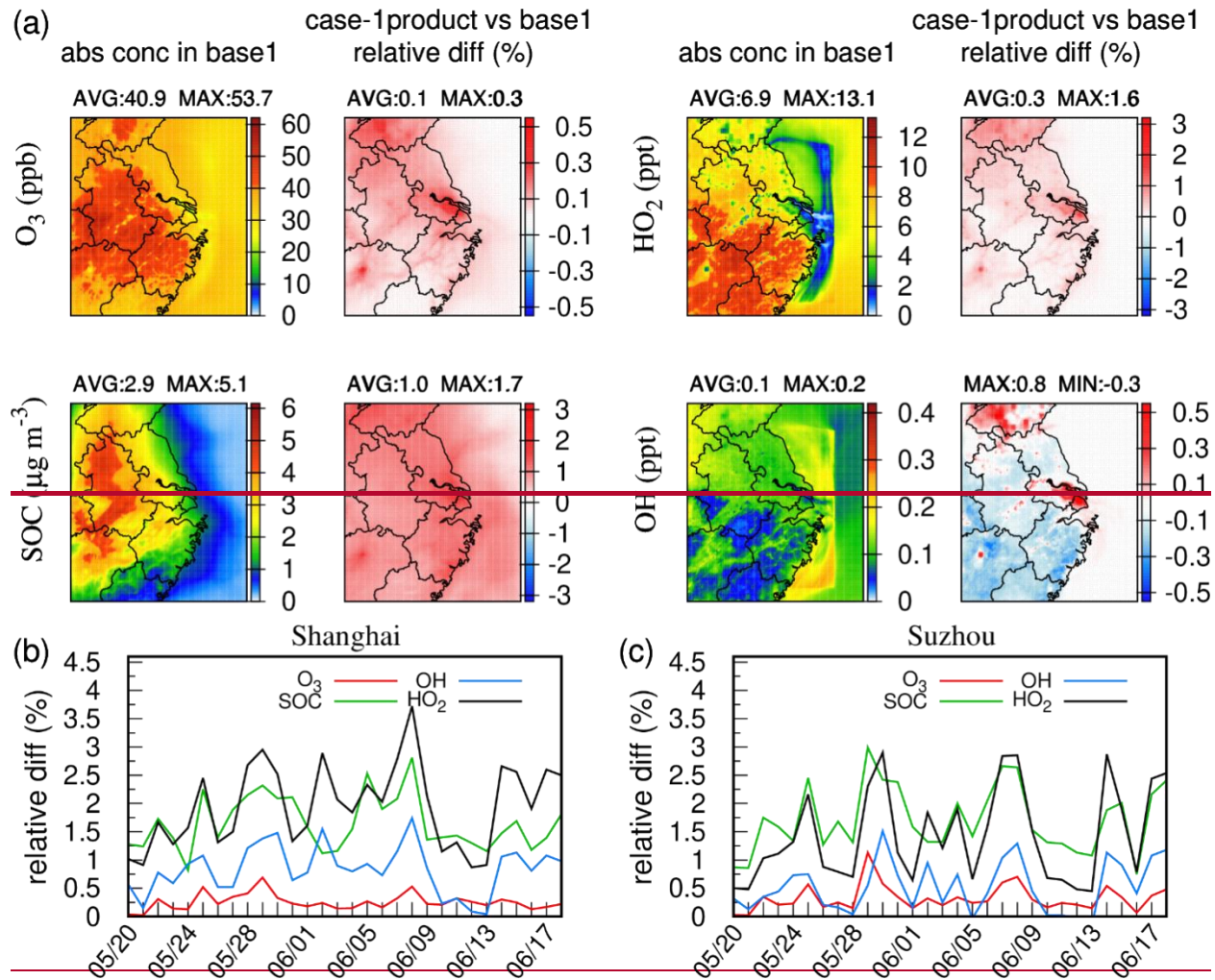


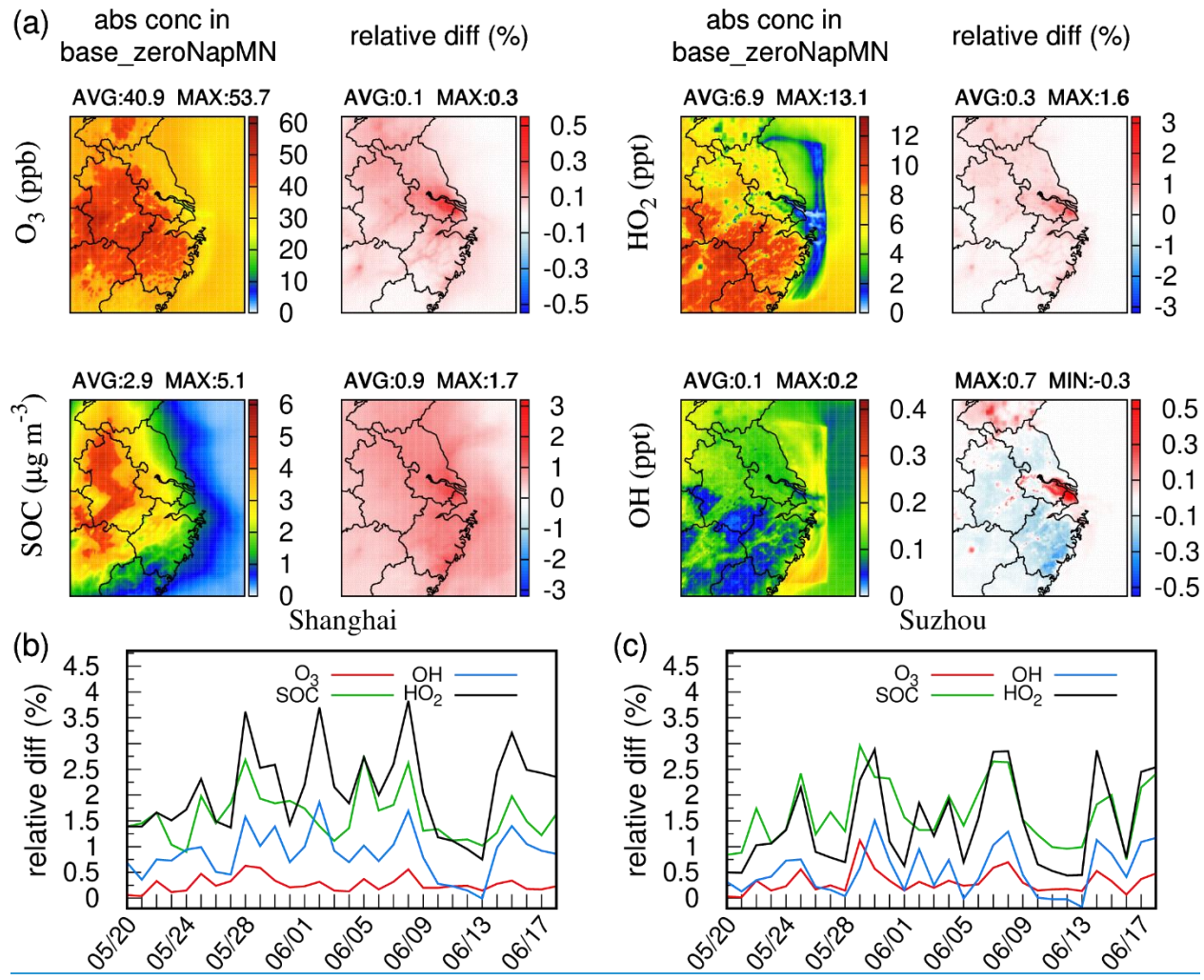
760



761

762 **Figure 34.** Contributions of the major aromatic species to (a) the total emissions of aromatics  
 763 (weight fraction) and the aromatic-derived SOC in (b) case-1 product and (c) case-2 products at the  
 764 Taizhou site. ~~These~~ The aromatic species ~~are~~ include Nap, 1-MN, 2-MN, BENZ, the sum of toluene  
 765 and aromatics with  $k_{OH} < 2 \times 10^4 \text{ ppm}^{-1} \text{ min}^{-1}$  (ARO1+TOLU), and the sum of xylenes, 1,2,4-  
 766 trimethyl benzene and aromatics with  $k_{OH} > 2 \times 10^4 \text{ ppm}^{-1} \text{ min}^{-1}$  excluding Nap and MN  
 767 (ARO2MN'+MPO+B124).





771 **Figure 45.** (a) AbsoluteAverage concentrations of SOC,  $O_3$ ,  $OH$ , and  $HO_2$  in  
772 base1, base\_zeroNapMN and changes in case-1product relative to base1,  
773 respectively, base\_zeroNapMN. Daily relative changes in case-1product compared to base1  
774 at base\_zeroNapMN in (b) Shanghai and (c) Suzhou.